

Engineering Conducting Polymer Hydrogels for Bioelectronic Interfacing

Yu Xue, Zhipeng Ni, Yafei Wang, Liangjie Shan, and Ji Liu*

Bioelectronics promise transformative advances in healthcare through seamless tissue-device integration, yet fundamental mismatches persist between the soft, hydrated nature of biological systems and the rigid, anhydrous architecture of conventional electronics, manifesting as mechanical incompatibility, electrochemical decoupling, and chronic foreign body responses. Conducting polymer hydrogels (CPHs) uniquely mediate this divide by synergizing hydrogel-like tissue compliance and hydration with tunable mixed ionic-electronic conductivity, enabling applications from conformal electronic skins to implantable biosensors. While CPHs have demonstrated progress in reducing interfacial impedance and mechanical mismatch, the field lacks systematic frameworks correlating molecular design with dynamic performance under physiological loading. This review consolidates advances in CPH engineering, from foundational structure-property relationships to scalable fabrication techniques like 3D printing and photolithography, while critically evaluating emerging applications in closed-loop theranostics and highlighting unmet challenges in long-term stability and multimodal signal fidelity. By bridging materials innovation with clinical translation paradigms, the analysis provides a roadmap for next-generation bioelectronics that harmonize with living systems across spatiotemporal scales.

1. Introduction

Bioelectronic interfaces with living organisms have become an optimal platform for acquiring diverse physiological data and modulating physiological activities in real-time and everyday contexts.^[1–3] The seamless integration of the human body with bioelectronic devices accelerates the advancements in human-machine interaction, neuroscience, and artificial intelligence, which have also offered a foundation for deepening our understanding of complex physiological processes.^[2,4,5] Since the invention of the first artificial pacemaker, numerous wearable and implantable bioelectronics have been developed to monitor electrophysiological signals from various organisms and disease

treatment.^[6–8] The advent of these bioelectronics has brought unprecedented opportunities for accurate diagnosis and efficient therapeutics for various diseases and disorders such as Parkinson's disease, cerebral stroke, and cardiovascular diseases.^[1,7,9] Despite recent advancements, the intrinsic dissimilarities between living organisms and bioelectronic devices have posed significant challenges in terms of biocompatibility, dramatic mismatch in electrical and mechanical attributes, as well as long-term reliability, thus hampering the rapid progress and implementation of bioelectronic technologies.^[1,2,10,11]

Conventional electronics, crafted from rigid and abiotic materials like metals and silicon, exhibit intrinsic incompatibility with biological tissues.^[1,10] Furthermore, biological systems adeptly convey complex and dynamic signals via hydrophilic carriers like ions and biomolecules, unlike conventional electronics rely on the controlled conduction of electrons and holes.^[10,12] These discrepancies result in interfacial discontinuities, adverse foreign body reactions, and fibrotic encapsulation, thus severely impairing the bioelectronic efficacy.^[1,2,13] To address these challenges, researchers are diligently exploring soft, wet, ion conducting and biocompatible materials to seamlessly bridge the gap between bioelectronic devices and living organisms.^[10,14] In light of their tissue-like mechanics, high-water content, ionic environment, and biocompatibility, hydrogels are emerging as ideal interface materials for the seamless integration between living organisms and electronic devices.^[10,15] Traditional hydrogels, relying on ionic conduction, suffer from low electrical conductivity ($<1\text{ S m}^{-1}$), and are always accompanied with inferior bioelectronic interfacing.^[16–18] The incorporation of a spectrum of nanomaterials, including metallic nanoparticles, carbon nanotubes, and graphene, within hydrogels could markedly increase their electron conductivity.^[19,20] However, the substantial disparities in surface energy and dimension between the nanoscale hydrophobic conducting fillers and the hydrophilicity polymer chains in hydrogel networks, along with potential biotoxicity, poses major challenges for the high-fidelity and reliable bioelectronic interfacing.^[14,16]

Unlike traditional conducting materials, conducting polymers (CPs), such as polypyrrole (PPy), polyaniline (PANI), and poly(3,4-ethylenedioxythiophene) (PEDOT), differ fundamentally from traditional conductors by enabling dual

Y. Xue, Z. Ni, Y. Wang, L. Shan, J. Liu
 Department of Mechanical and Energy Engineering
 Southern University of Science and Technology
 Shenzhen 518055, China
 E-mail: liuj9@sustech.edu.cn

 The ORCID identification number(s) for the author(s) of this article can be found under <https://doi.org/10.1002/adfm.202521327>

DOI: 10.1002/adfm.202521327

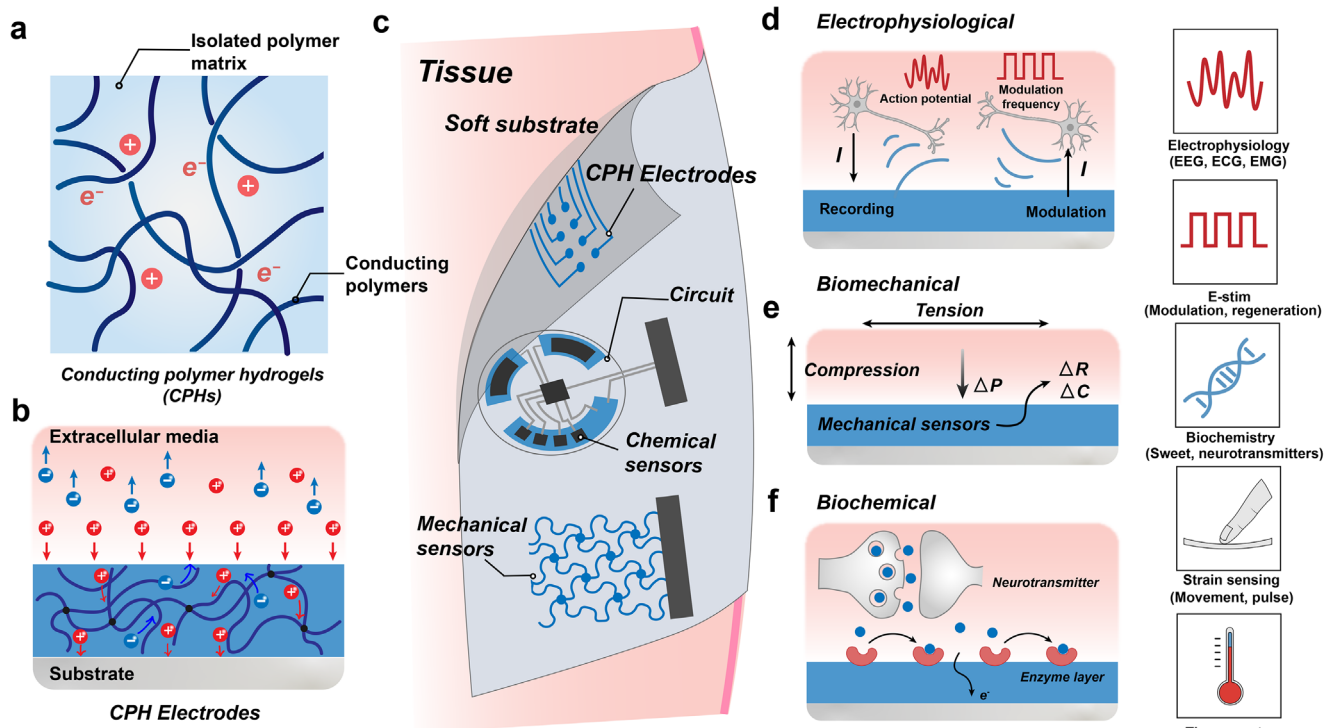


Figure 1. Conducting polymer hydrogels (CPHs) for bioelectronic interfacing. a) CPHs synergistically integrate the merits from both hydrogels (soft, high-water content and biocompatibility) and conducting polymer (hybrid ion- and electron-conducting capability). b) Schematic illustration of coating metallic electrodes with CPHs, endowing the electrodes with decreased interfacial impedance, accessible electron and ion conductivity, high-water content (>70%) and mechanical compliance. c–f) Schematic illustration of CPHs-based bioelectronics for the high-fidelity interfacing with the human body (c), including electrophysiological monitoring (d), biomechanical sensing and modulation (e), and also sensing of biological chemicals, temperature and body movement (f).

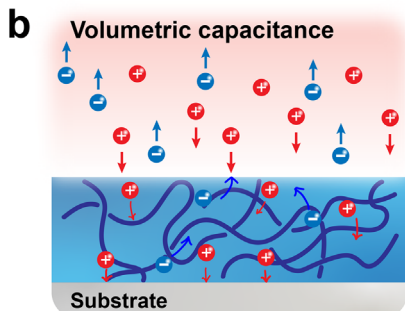
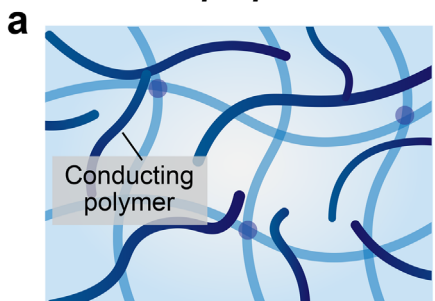
ionic-electronic conductivity, which reduces interfacial impedance for efficient ion-to-electron transduction at bioelectronic interfaces.^[9,21,22] The organic and polymeric backbones of CPs confer compatibility with hydrogel matrices, enabling the formation of conducting polymer hydrogels (CPHs) that synergistically combine the advantages of both constituents (Figure 1a).^[21,23] By leveraging the complementary ionic and electronic conduction pathways derived from the CPs, CPHs exhibit conductivities (10^2 – 10^5 S m $^{-1}$) that substantially surpass those of conventional polymer hydrogels (10^0 – 10^2 S m $^{-1}$).^[17] Owing to their exceptional combination of chemical, mechanical, and electrical properties, CPHs have attracted significant interest for biomedical applications (Figure 1b). These applications include wearable and implantable devices for electrophysiological recording, biosensing, and electrical stimulation (Figure 1c–f).^[14,24] Current research prioritizes enhancing CPHs' mechanical resilience, electrical stability, and multifunctionality (e.g., self-healing, tissue adhesion) while exploring novel material formulations.^[16,25,26] Despite these advances, a comprehensive understanding of the unique attributes and design principles of CPHs for bioelectronic interfaces remains limited. Further development is needed to optimize these materials for high-fidelity bioelectronic interfacing, thereby improving electrophysiological monitoring, stimulation efficacy, and long-term stability. Such progress is essential for advancing clinical bioelectronic applications and enabling next-generation bioelectronic interface

technologies. This review critically analyzes CPHs' unique advantages in bioelectrical interfacing, proposes design principles for high-performance materials/devices, and explores strategies to bridge artificial electronics with living systems through tailored interface engineering. By elucidating structure-function relationships and integration challenges, the discussion aims to advance clinical-grade bioelectronic technologies capable of seamless biotic-abiotic synergy.

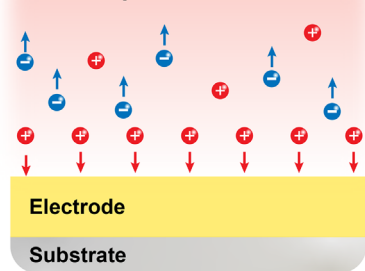
2. Engineering Conducting Polymer Hydrogels (CPHs) with Distinct Attributes

CPHs outperform traditional metal/silicon-based electrodes in terms of electrical and electrochemical characteristics, arising from the unique hybrid ion- and electron conducting capability (Figure 2a–c).^[14] CPHs with tissue-like modulus could be applied conformably onto biological tissues, thus effectively alleviating those immunological rejection and inflammatory responses (Figure 2d–f).^[16] The remarkable biocompatibility of CPHs, along with their porous and hydrophilic structure, enhances cellular interactions, reduces inflammation, and promotes immune tolerance. Additionally, it could also enable the effective diffusion of biomolecules and removal of metabolites to optimize cellular functions, which are crucial for biological signaling (Figure 2g,h).^[10] Besides, the biodegradability can be

Electrical properties

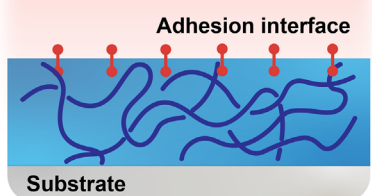


Areal capacitance

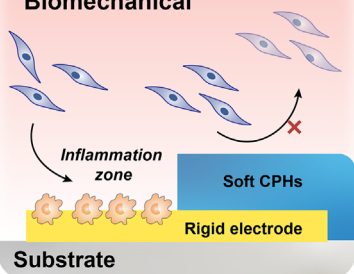


Mechanical properties

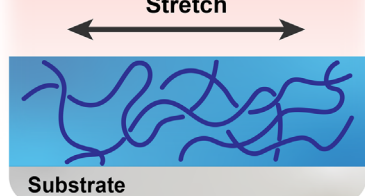
d Adhesion



e Biomechanical

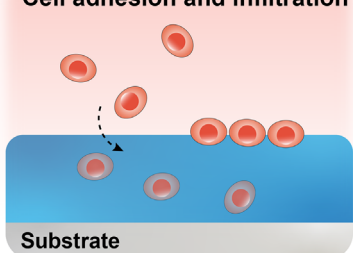


f Stretchable

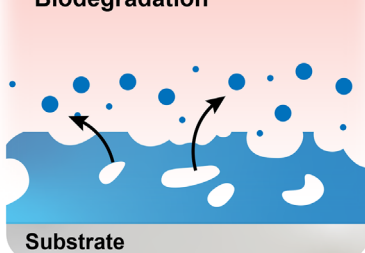


Biological properties

g Cell adhesion and infiltration



h Biodegradation



i Diffusion of biomolecules

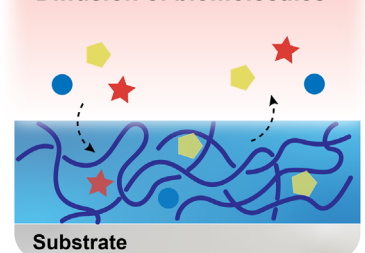


Figure 2. Engineering CPHs with unique attributes for bioelectronic interfacing. a–c) CPHs possess a combination of ionic and electronic conductivity, enabling the high-fidelity bioelectronic interfacing between the electronics and human body. The capacitive charge injection via a CPHs electrode relies on the establishment of a molecular-level electrical double layer (EDL) spanning the entire hydrogel, and the capacitance is proportional to the volume of the CPHs electrode (termed as volumetric capacitance, b). For pure metallic electrode, the capacitive charge injection is contingent upon surface-based EDL, with capacitance correlating directly to electrode's surface area (termed as areal capacitance, c). d–f) CPHs possessing tissue-like mechanics enable conformal adhesion to biological surfaces (d), diminish the risk of immunological rejection and inflammation (e), and synchronously adapt to tissue deformation (f). g–i) The high-water content and exceptional biocompatibility of hydrogel network impart the CPHs with improved cellular interaction (g), diffusion of biomolecules and elimination of metabolites (h), and biodegradability through chain engineering (i).

tailored through the use of materials like chitosan and gelatin from natural and synthetic sources (Figure 2i).

2.1. Electrical Properties

Biological tissues function as ionic electrolyte conductors, where variations in ion channel density and structural organization create tissue-specific electrical properties—cardiac tissue achieves high conductivity ($\approx 0.5 \text{ S m}^{-1}$) through gap junctions and Purkinje fiber networks that enable rapid signal propagation, whereas skin exhibits layer-dependent conductivity with the stratum corneum acting as a low-conductivity barrier ($\approx 0.01 \text{ S m}^{-1}$) and hydrated dermal/subcutaneous layers showing moderate conductivity ($0.01\text{--}0.1 \text{ S m}^{-1}$).^[27] These intrinsic variations necessitate CPHs with tunable electrical characteristics to ensure bioelectronic compatibility, enabling precise impedance matching and efficient signal transduction at dynamic electrode-tissue interfaces. By tailoring CPHs properties to mimic target tissue conductivity, this adaptive strategy overcomes the fundamental challenge of maintaining stable, high-fidelity bioelectronic performance across diverse physiological environments.

The electrode-tissue interface constitutes the critical cornerstone of bioelectronic systems, serving as the primary gateway for bidirectional signal transduction.^[2] This interface facilitates

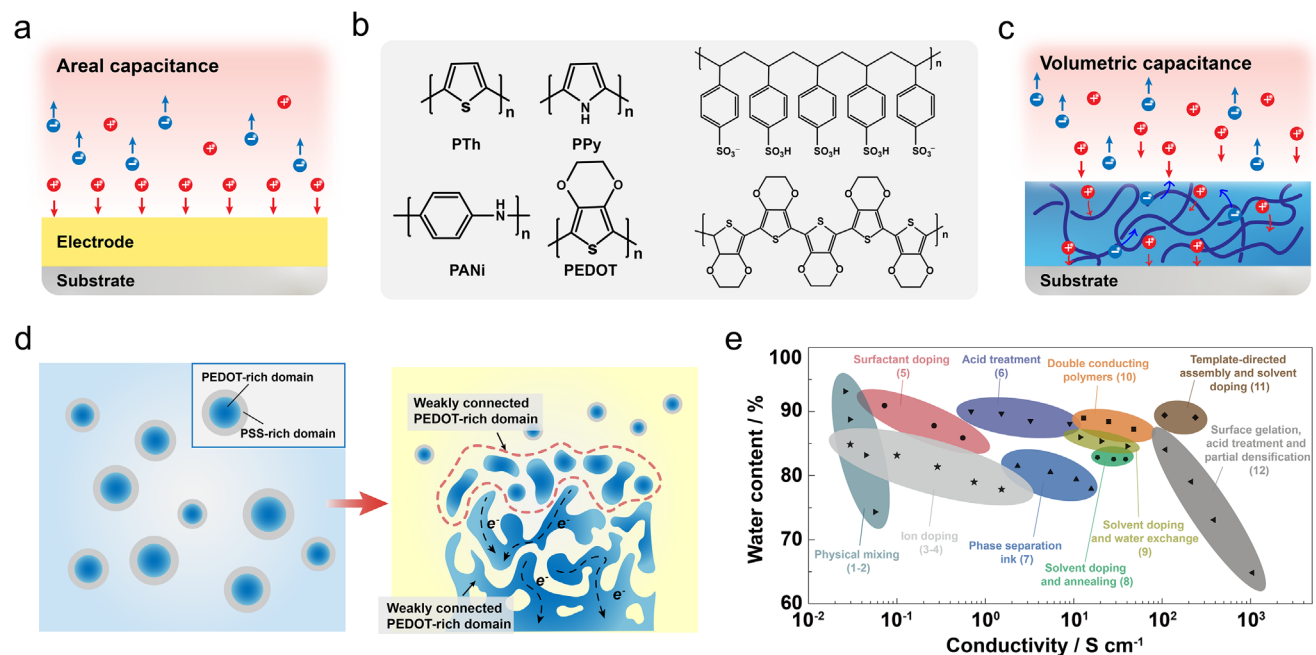


Figure 3. Design rationales for CPHs with tailored electrical properties. a) For metallic electrode, the capacitive charge injection is contingent upon surface-based electrical double layer (EDL), with capacitance correlating to electrode's surface area (termed as areal capacitance). b) Representative chemical structures of commonly-used CPs. c) The charge injection via a CPHs electrode relies on the establishment of a molecular-level EDL spanning the entire hydrogel, with capacitance proportional to the volume of the CPHs electrode (termed as volumetric capacitance). d) Schematic illustration of chemically-triggered phase separation of PEDOT:PSS, followed by segregation of the PEDOT domains, leading to the increase in electrical conductivity. e) Comparison chart by plotting water content and conductivity for PEDOT:PSS-based CPHs. Data of PEDOT:PSS-based hydrogels prepared from different strategies (physical mixing,^[31,32] ion doping,^[33,34] surfactant doping,^[35] acid treatment,^[36] phase separation ink,^[24] solvent doping and annealing,^[37] solvent doping and water exchange,^[38] double CP,^[39] template-directed assembly and solvent doping,^[40] surface gelation, acid treatment and partial densification^[41] were compiled from previous reports.

the precise capture of endogenous biological signals (e.g., action potentials, local field potentials, and electrochemical changes) for diagnostic monitoring and neuroscientific investigation.^[28] Concurrently, it enables the targeted delivery of exogenous electrical stimuli to modulate neural activity, restore sensory or motor function, or provide therapeutic interventions for a range of neurological and physiological disorders.^[28,29] To enhance the efficacy of both bioelectronic recording and stimulation, it is imperative to engineer electrodes with superior electrochemical performance. Key performance metrics include a low interfacial impedance, which is essential for maximizing the signal-to-noise ratio (SNR) during recording by minimizing thermal noise and signal attenuation at the interface.^[30] Equally critical is a high charge injection capacity (CIC), which dictates the maximum amount of charge that can be safely delivered into the tissue during a stimulation pulse without causing irreversible electrochemical reactions or tissue damage.^[30] Furthermore, a high charge storage capacity (CSC) reflects the total charge available for injection, influencing the device's ability to deliver sustained or high-frequency stimulation protocols.^[14,30] Despite the prevalent use of miniaturized metal and silicon-based bioelectrodes, their double-layer capacitor nature is accompanied with high electrochemical impedance ($>1000 \text{ M}\Omega \text{ }\mu\text{m}^{-2}$ at 1 kHz) and low CIC ranging from 0.01 to 0.5 mC cm⁻², alongside with a CSC of 0.1 to 1 mC cm⁻² (Figure 3a).^[14] Such inferior electrochemical properties can compromise the signal transduction efficiency, and further deteriorate the stimulation and recording efficacies.^[30]

The electronic conductivity of conducting polymers (CPs) originates from delocalized π -electrons in their conjugated backbones, enabling efficient charge transport through continuous molecular pathways (Figure 3b).^[31] A defining feature of CPs is their ability to be doped with ions, a process that allows their electronic conductivity to be precisely tuned across a wide spectrum, from semiconducting to near-metallic levels.^[9,22] This dual ionic/electronic conductivity is paramount, as it enables the CPs-based electrode to seamlessly couple with the ionic, charge-carrier environment of biological tissues, thereby facilitating a more efficient and biocompatible signal transduction at the electrode-tissue interface.^[42] Additionally, the inherent hydrophilicity of CPs allows them to absorb significant amounts of water, forming a hydrogel state that is exceptionally well-suited for interfacing with the aqueous biological environment.^[37] The high water content creates a percolating network that facilitates rapid ion permeation and transport throughout the CPHs matrix, effectively mimicking the ionic conductivity of native tissue.^[17] Concurrently, the intertwined CPs backbones establish a continuous, 3D electronic pathway. Crucially, this nanostructured architecture results in the formation of nanoscale or sub-nanoscale molecular-level electrical double layers (EDLs) distributed across the entire hydrogel volume, rather than being confined to a planar electrode surface.^[14] This volumetric capacitance effect dramatically increases the effective surface area available for charge exchange.^[41] The resulting synergy between the continuous electronic transport pathway and the pervasive ionic transport

network profoundly enhances overall charge dynamics and supports highly efficient, reversible Faradaic reactions.^[14] These combined properties are essential for establishing a stable, high-efficiency, and low-impedance bioelectronic interface, which is paramount for achieving sensitive signal recording and safe, effective stimulation over extended periods.

The PEDOT:PSS hydrogel stands out as a promising material for bioelectronic interfaces, demonstrating superior electrochemical performance, notably an electrochemical impedance below $< 100 \text{ M}\Omega \text{ }\mu\text{m}^{-2}$ (at 1 kHz) and a CSC exceeding 10 mC cm^{-2} .^[30,43] Critically, its CIC ($>3 \text{ mC cm}^{-2}$) substantially surpasses that of conventional rigid electrodes, such as noble metals and carbon-based materials, positioning it as a superior candidate for safe and effective electrical stimulation.^[2,30,43] Generally, the PEDOT short chains ($M_n < 1,000 \text{ g mol}^{-1}$) are initially complexed with the long-chain PSS ($M_n > 400,000 \text{ g mol}^{-1}$), forming nanoscale micelles in an aqueous environment.^[44,45] Such kind of micellar structure physically obstructs the formation of a continuous, percolating conductive pathway, thereby constraining the bulk electrical conductivity of the hydrogel to relatively low levels, often $\approx 0.1 \text{ S m}^{-1}$.^[46] Various strategies, including chemical (e.g., organic solvents, surfactants, and ionic liquids) and physical treatments (e.g., annealing and laser), have been deployed to enhance the conductivity of PEDOT:PSS-based hydrogels.^[46,47] These approaches are harnessed to induce the phase separation and rearrangement of PEDOT and PSS chains within the hydrogel matrixes (Figure 3d), resulting in a substantial increase in the conductivity, from 0.1 to $\approx 10^5 \text{ S m}^{-1}$ (Figure 3e).

2.2. Mechanical Properties

Biological systems are inherently dynamic and heterogeneous, exhibiting a wide spectrum of mechanical properties that range from the soft, pliable nature of brain tissue (modulus in the kilopascal range) to the much stiffer tendons and bone (modulus in the gigapascal range).^[14,48] Both the tissues themselves and any interfacing electronic devices experience a dynamic spectrum of mechanical deformations during physiological activities, encompassing everything from the subtle strains of pulsatile blood flow and the cyclical stretching of muscle contraction and joint articulation, to the more vigorous forces of daily movement and external impacts.^[2,49] An optimal epidermal electrode must be engineered to closely emulate the mechanical properties of the skin, including its low elastic modulus, high compliance, and viscoelastic behavior.^[50] Such mechanical compliance is paramount for achieving a conformal, seamless, and robust interface with the underlying biological system.^[11,19,51] This intimate physical coupling ensures the electrode's stability and reliable signal transduction during periodic and vigorous epidermal deformations, such as bending, stretching, and twisting, thereby enabling high-fidelity monitoring without motion artifacts or causing discomfort to the wearer.^[4]

The challenge of mechanical compatibility is even more pronounced for implantable bioelectronics, which operate in a more demanding and complex physiological environment.^[13,31] These devices are perpetually susceptible to a variety of mechanical stresses, including static strains from tissue encapsulation and

dynamic forces from organ movement.^[2,7,13] This chronic mechanical loading can lead to a cascade of detrimental effects: the gradual deterioration of interfacial stability as the device loosens or forms a fibrotic capsule; a compromise in biocompatibility, triggering chronic inflammation or foreign body responses; and a degradation of electrochemical performance due to micro-crack formation or delamination of the active materials.^[2,13]

CPHs retain the intrinsic softness of hydrogel materials, conferring distinct advantages in mediating biomechanical interactions at the tissue-electrode interface (Figure 4a). However, conventional pure CPHs suffer from poor stretchability ($< 10\%$) and toughness ($< 100 \text{ J m}^{-2}$), arising from the intrinsic brittleness of the CPs-rich domains (Figure 4b).^[10] Recently, numerous strategies have been developed to endow CPHs with superior mechanics, including stretchability, toughness and fatigue resistance. For instance, by incorporating energy dissipation moieties within the CPHs networks,^[25] the reversible dissociation and association of those dynamic interactions can substantially dissipate energy to prevent interfacial and/or bulk fractures, leading to CPHs with high toughness (Figure 4c). This attribute is particularly vital for bioelectronic interfaces, as it guarantees the integrity of the interface even under severe mechanical deformations stress or external impacts.^[52] The tailoring of these mechanical properties facilitates the optimization of hydrogel integration with the target tissue, thereby reducing the potential for mechanical mismatches that could lead to chronic inflammation or tissue damage. Spontaneously achieving high fracture toughness and superior electrical conductivity in CPHs presents a challenge, as the inclusion of flexible yet insulating polymer backbones (*i.e.*, polyacrylamide) may destroy the connectivity of the conducting phases within the hydrogel matrix.^[32] By creating bi-continuous CPHs using phase-separated ink, the continuous phase of PEDOT:PSS imparted the hydrogel with high conductivity ($\approx 1100 \text{ S m}^{-1}$), whereas the continuous PU phase contributed to a fracture toughness as high as 3300 J m^{-2} .^[32] This simultaneous improvement in electrical and mechanical properties helps to overcome the critical trade-off between conductivity and toughness, enabling the development of reliable CPHs-based bioelectronics for chronic applications.

Although incorporation of energy dissipation moieties could markedly enhance the toughness of CPHs, they are still susceptible to fatigue fracture when they are exposed to long-term periodical mechanical loading. The fatigue threshold, defined as the minimal fracture energy required for crack propagation under cyclic loading, is quantified as low as 10 J m^{-2} for PEDOT:PSS-based CPHs.^[53] Inspired by the finding that intrinsically high-energy phases (such as nanocrystalline domains and preferentially aligned micro/nano fibers) can effectively pin fatigue crack propagation (Figure 4d),^[54] Lu et al. engineered CPHs using a combined strategy of freeze-casting and nanocrystalline domain engineering. The resulting CPHs, featuring a preferentially aligned structure, exhibited a remarkable fatigue threshold exceeding 300 J m^{-2} (Figure 4e).^[53] Such superior fatigue resistance can effectively pin the crack propagation within the CPHs (Figure 4f) during over 1000000-cycle dynamic mechanical loading at an applied energy release rate of 300 J m^{-2} , ensuring long-term stability within the dynamic biological environment. Such design rationale could be readily applied to fabricate fatigue-resistant CPHs of various chemical formulations. Additionally, these CPHs retained a low Young's modulus ($\approx 100 \text{ kPa}$)

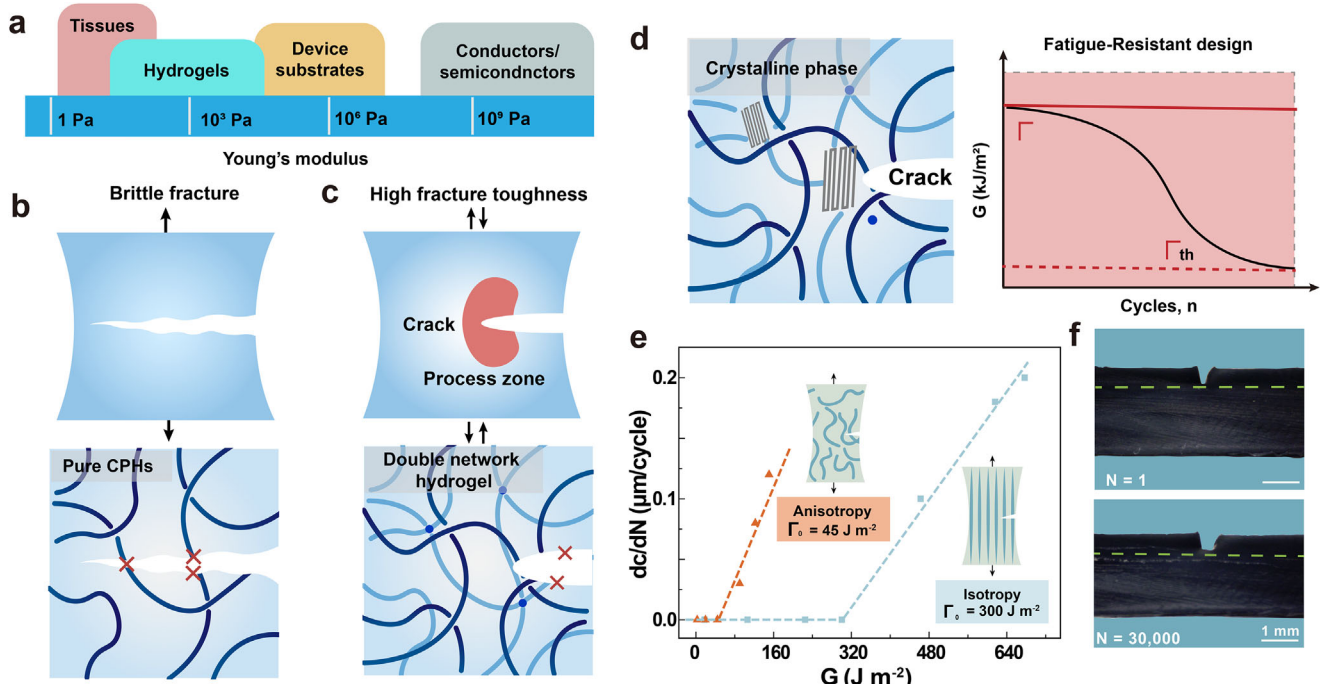


Figure 4. Design rationales for CPHs with tailored mechanical properties. a) Schematic illustration for the mechanical similarity between CPHs and biological tissues. b) Brittle fracture of conventional CPHs featuring toughness below 10 J m^{-2} . c) Engineering CPHs with high toughness by incorporating energy dissipation moieties, such as formation of double network structure with the CPHs matrix. d) Engineering CPHs with fatigue-resistant by incorporating intrinsically high-energy domains (i.e., nanocrystalline domains) within the CPHs matrix. Presence of nanocrystals could effectively pin the fatigue crack propagation during the long-term periodical mechanical loading. e) Anisotropic fatigue-resistance property of the CPHs, with significantly increased fatigue threshold along the alignment direction. f) Images recording the crack propagation of the CPHs during 30000 cycle tensile test verification at an energy release rate of 300 J m^{-2} . e,f) Reproduced with permission from ref.[52] Copyright 2023 Wiley-VCH.

and a high-water content ($\approx 86.7 \text{ wt.\%}$), making them a promising material for dynamic biointerfacing.

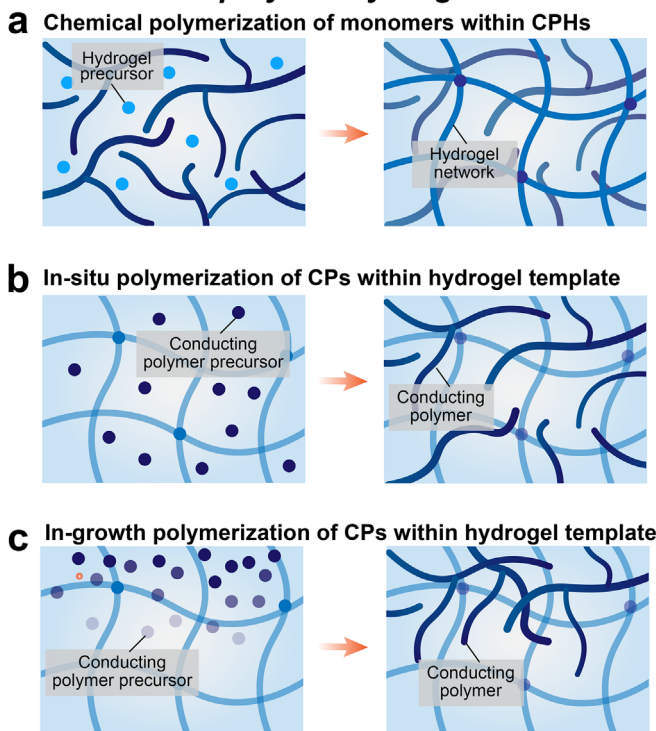
2.3. Biological Properties

Ensuring the biocompatibility of bioelectronics is essential for their long-term reliable functionality, particularly for implantable devices that are more invasive. The biocompatibility of these devices encompasses several key aspects: chemical non-toxicity to preclude the release of harmful leachables, mechanical compatibility to avert tissue damage, and favorable biological interactions to prevent adverse reactions.^[55] The employment of inappropriate interface materials can elicit chronic inflammation, compromise neuronal function, and impair device performance like increasing interfacial impedance, elevating signal noise, degrading signal quality, and reducing stimulation efficiency.^[2] The exceptional biocompatibility of CPHs has been extensively validated and underpins their widespread applications in tissue engineering, wound healing, and bioelectronics.^[17] Chemically, CPHs are primarily composed of biocompatible CPs and other long-chain polymers, ensuring the absence of toxic leachables.^[56] A significant challenge in enhancing the conductivity of PEDOT:PSS hydrogels is that the required dopants can compromise biocompatibility. Typically, these potentially toxic substances can be removed through solvent rinsing, or alternatively, biocompatible additives can be employed.^[40] For instance, the incorporation of D-sorbitol,

a nutritive sweetener, as a non-toxic additive yields soft, stretchable PEDOT:PSS hydrogels that simultaneously achieve high conductivity ($\approx 7000 \text{ S m}^{-1}$) and excellent biocompatibility, evidenced by the absence of significant inflammatory response following nine weeks of *in vivo* implantation.^[57] In terms of mechanical attributes, CPHs exhibit tissue-like soft properties, facilitating seamless integration with host tissue and minimizing mechanical trauma or discomfort, which in turn helps to reduce inflammation and the foreign body response.^[58] Moreover, the porosity and hydrophilicity of CPHs allow for the diffusion of essential biomolecules, such as oxygen and nutrients, while facilitating the removal of waste products. Given the unique biocompatibility of CPHs, it can promote cellular activities, including cell adhesion, migration, proliferation, differentiation, and protein secretion, which are crucial for biological signal transduction.^[59] Especially interfacial materials of neuroelectronic hybrid systems that feature both, ion and electron conduction as well as a direct conversion between both conducting types, while enabling a low liquid-solid interface impedance, offer outstanding properties for the development of high-performance bioelectronic devices.

The biodegradability of CPHs addresses chronic implantation risks by integrating CPs with degradable polymers (proteins, polysaccharides, synthetic analogues) that hydrolyze, enzymatically degrade, or undergo cell-mediated breakdown into metabolizable byproducts.^[60] While CPs themselves resist metabolic degradation, their nanostructured composites enable macrophage-mediated phagocytosis and renal clearance.^[10] For

Interpenetrating network conducting polymer hydrogels



Pure conducting polymer hydrogels

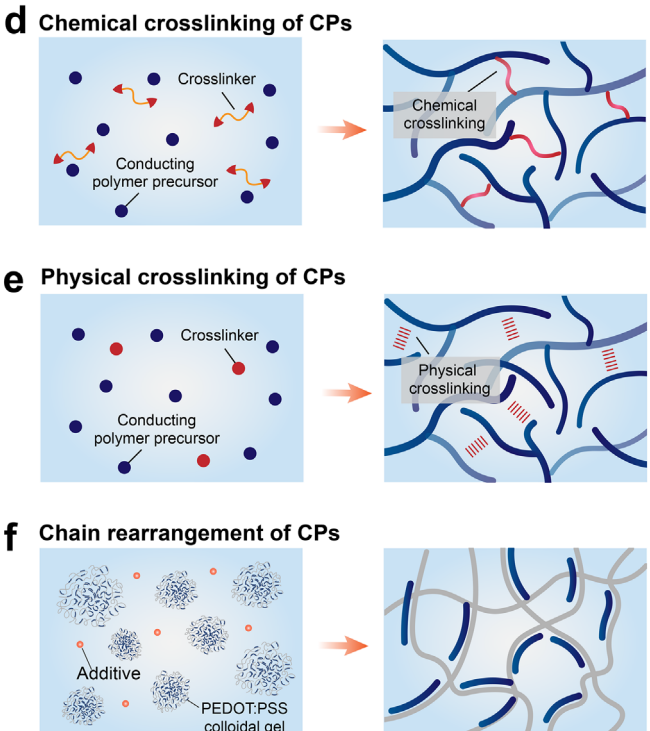


Figure 5. Synthesis strategies of CPHs. a–c) CPHs with IPN structure are typically prepared through three major approaches: co-polymerization of CPs with another flexible and non-conducting hydrogel backbone (a), in situ polymerization of CP precursors (i.e., EDOT) within another hydrogel network (b), and in-growth polymerization of CP precursors into another hydrogel network (c). d–f) Schematic illustration for pure CPHs fabricated in the absence of another hydrogel network, through chemical (d) or physical (e) crosslinking routines, as well as chain rearrangement (f).

instance, CPHs-based electrodes prepared from PEDOT and gelatin provide a cytocompatible electrophysiological environment similar to that of natural neural tissue, which enhances neural cell adhesion, growth, and signal transduction.^[61] Moreover, these CPHs-based electrodes exhibit substantial degradation within 28 days under physiological conditions without releasing neurotoxic degradation products. This dual capability, preserving bioelectronic functionality during service life while ensuring controlled post-operative resorption, positions CPHs as a transformative platform for biocompatible bioelectronics, balancing tunable degradation kinetics with interfacial stability for chronic neural interfacing.

3. Fabrication and Manufacturing Strategies

3.1. Fabrication Strategies of High-Performance CPHs

Various methods have been employed in the synthesis of CPHs. Typically, CPHs are prepared by forming molecular-level composites or interpenetrating networks (IPNs) through the integration of CPs with another flexible hydrogel matrices. Recently, the focus has shifted toward developing pure CPHs, composed entirely of CPs, thus removing the need of non-conductive hydrogel templates to sacrificing electrical performance. In the following sections, we delve into the latest advancements in the field of CPHs, focusing on two primary preparation strategies.

3.1.1. Interpenetrating Network CPHs

Directly mixing CPs with other flexible polymers, including natural polymer (e.g., collagen, hyaluronic acid, alginate, chitosan) or synthetic polymer (e.g., polyacrylamide, poly(acrylic acid), poly(vinyl alcohol)), is a straightforward and simple approach to forming CPHs.^[62] However, excessive hydrophobic CPs may form aggregates within the hydrogel due to thermodynamic incompatibility, thus leading to fragmented conducting pathways, as well as compromised electronic conductivity (below 1 S m^{-1}) and mechanical properties (strain below 50%).^[17] To address the challenge, one representative solution is to pre-establish CPs networks before polymerizing the hydrophilic hydrogel precursors to fabricate CPHs featuring an interpenetrating network (IPN) structure (Figure 5a). The IPN consists of two or more interpenetrated polymer networks, which are individually cross-linked but not joined together. CPs are commonly integrated into the hydrogel network through physical entanglement.^[54,63] The IPN design of CPHs is advantageous as it facilitates the demonstration of extraordinary mechanical performance, attributed to the robust interpenetrating network entanglement and efficient energy dissipation.^[36] CPHs with IPNs were fabricated by infiltrating acrylic acid into a loosely crosslinked PEDOT:PSS gel, followed by polymerization to form a PAA network. This strategy could effectively preserve the conducting network's integrity and resulting in CPHs with high deformation capacity (strain $\approx 400\%$) and con-

ductivity (23 S m^{-1}).^[64] Additionally, *in situ* oxidative polymerization of CPs precursors within a non-conducting hydrogel matrix has also been used to fabricate CPHs with an IPN structure. This approach can enhance mechanical properties by taking advantage of the chain's entanglement between CPs and the flexible network (Figure 5b).^[42,65,66]

Moreover, the synthesis of CPHs can also be achieved via electropolymerization. (Figure 5c). Liu et al. has successfully fabricated CPHs by first chemically grafting functional long-chain polymers, poly(styrene sulfonate-*co*-4-vinyl pyridine) (poly(SS-4VP)), onto metallic substrates, then electrochemically depositing CPs, and finally chemically cross-linking them to form a PEDOT:Poly(SS-4VP) IPNs. Such CPHs coating exhibit tissue-like modulus ($\approx 800 \text{ kPa}$), robust interface, highly-desirable electrochemical properties (a decrease of $\approx 9\%$ in CSC after 10000-cycle scanning), and long-term reliability.^[67]

3.1.2. Pure CPHs

Unlike other conducting fillers (e.g., metallic or carbon nanomaterials), the organic and polymeric nature of CPs allows the formation of hydrogels themselves even in the absence of additional hydrophilic polymers.^[37] These hydrogels, known as pure CPHs, are typically created by direct cross-linking of conducting chains to form a 3D network structure by covalent cross-linking or physical cross-linking. Chemical crosslinking is achieved by introducing chemically crosslinkable functional groups (e.g., carboxyl, amino) into CPs precursors, which further act as crosslinking sites of the final hydrogel networks (Figure 5d). Non-covalent crosslinking provides a versatile strategy for constructing pure CPHs, complementing traditional chemical approaches.^[68] Physical methods such as electrostatic interactions, polymer chain entanglement, and π - π stacking enable the development of CPHs with tailored functionalities, exemplified by the PEDOT:PSS/PANi system, where electrostatic self-assembly between oppositely charged polymers forms conductive networks ($\approx 0.7 \text{ S m}^{-1}$).^[69,70] The dynamic reversibility of these interactions allows stress-responsive bond dissociation and reformation, imparting self-healing, injectability, and energy dissipation for enhanced mechanical resilience. Supramolecular hydrogel integrate self-doped EDOT monomers into host-guest complexes (2BPyVI-CB[8]), achieving synergistic properties: stretchability ($>1000\%$), tissue-like softness (10.5 kPa), toughness (620 kJ m^{-3}), and conductivity (5800 S m^{-1}) through precisely engineered non-covalent crosslinking.^[42]

PEDOT:PSS stands out among these CPs as a unique composite with coexisting conjugated PEDOT and insulating PSS. The hydrophilic PSS imparts the PEDOT:PSS films with hydrogel-like properties in moist conditions, forming micellar structures with PEDOT-rich cores and PSS-rich shells.^[46] The molecular interactions in PEDOT:PSS, including electrostatic forces, π - π stacking, and interchain entanglements, can be adjusted to form an aqueously-stable network of PEDOT-rich domains within the PSS matrixes (Figure 5f).^[37] This unique architecture not only improves the water stability of the hydrogel but also endows it with mechanically tunable properties, making it a promising candidate for various applications in the fields of materials science and biotechnology.

3.2. Advanced Manufacturing of CPHs-Based High-Performance Bioelectronics

A range of advanced manufacturing techniques have been employed to fabricate CPHs-based bioelectronics, spanning nanometer to millimeter scales, to meet the specific demands of bioelectronics.^[21] These techniques ensure the precision and functionality of CPHs-based bioelectronics in the dynamic realm of biological systems. Screen printing is a cost-effective, operationally simple, and scalable technique for manufacturing various microelectronics (Figure 6a).^[57,71] Due to the constraints imposed by the screen mask and ink properties, screen printing is limited to planar processing of CPHs with a resolution of $\approx 200 \text{ }\mu\text{m}$, making it suitable for bioelectronics where high dimensional precision is not essential.^[72] Electrochemical polymerization is a well-established strategy for patterning CPs, typically involving the oxidation polymerization of monomers on electrode substrates. However, this method usually relies on conducting substrates, and the resulting CPHs typically exhibit a low water content (< 10%), leading to CPHs with modulus in the MPa range. A ionically induced gelation mechanism of patterning PEDOT:PSS with minimum feature sizes down to $100 \text{ }\mu\text{m}$ was addressed by using electrogelation, enabling the particles to aggregate and form gels stabilized by physical crosslink (Figure 6b).^[73] This method can fabricate CPHs with water content as high as 98.8%, resulting in extremely soft hydrogels with a modulus of $\approx 1 \text{ kPa}$, which closely matches that of soft biological tissues and minimizes mechanical mismatch at the tissue-device interface. Photolithography enables the creation of precise CPHs patterns through UV irradiation of a photoresist-coated substrate, where the resulting pattern serves as a mask for dry etching or as a sacrificial layer in wet etching (lift-off), facilitating the fabrication of complex circuits and microdevices.^[46,74] However, the highly porous structure and swelling behavior of CPHs limit the precision of patterned structures, typically resulting in feature sizes greater than $100 \text{ }\mu\text{m}$. Utilizing ionic liquids for doping PEDOT:PSS promotes the establishment of a networked architecture and enables the manipulation of swelling characteristics. Such CPHs could be further patterned with any desired geometries by photolithographic technology with a resolution down to $20 \text{ }\mu\text{m}$ (Figure 6c).^[38,74]

An alternative strategy, developed by Lu et al., leverages a hydrophilic, polyurethane-based, photocurable polymer as a photosensitive additive in the polymer ink to induce phase separation, yielding CPHs with co-continuous conducting and mechanical phases.^[74] These hydrogels exhibit excellent conductivity ($\approx 3000 \text{ S m}^{-1}$), exceptional electrochemical stability, a tensile strain of 50%, and high compatibility with high-resolution photolithography, allowing for the fabrication of features as small as $5 \text{ }\mu\text{m}$. Laser-assisted patterning, leveraging the capabilities of continuous-wave lasers to deliver intense electric fields and photothermal energy in an instant, has emerged as a cutting-edge method for fabricating high-performance CPHs-based bioelectronics.^[75] Utilizing this approach, the transformation of PEDOT:PSS into water-stable hydrogels has been achieved, leading to a remarkable spatial resolution of $6 \text{ }\mu\text{m}$ and an impressive electrical conductivity of $6.7 \times 10^4 \text{ S m}^{-1}$ (Figure 6d).^[75] Moreover, these hydrogels are completely sterile and free of toxic additives, eliminating the need for extensive

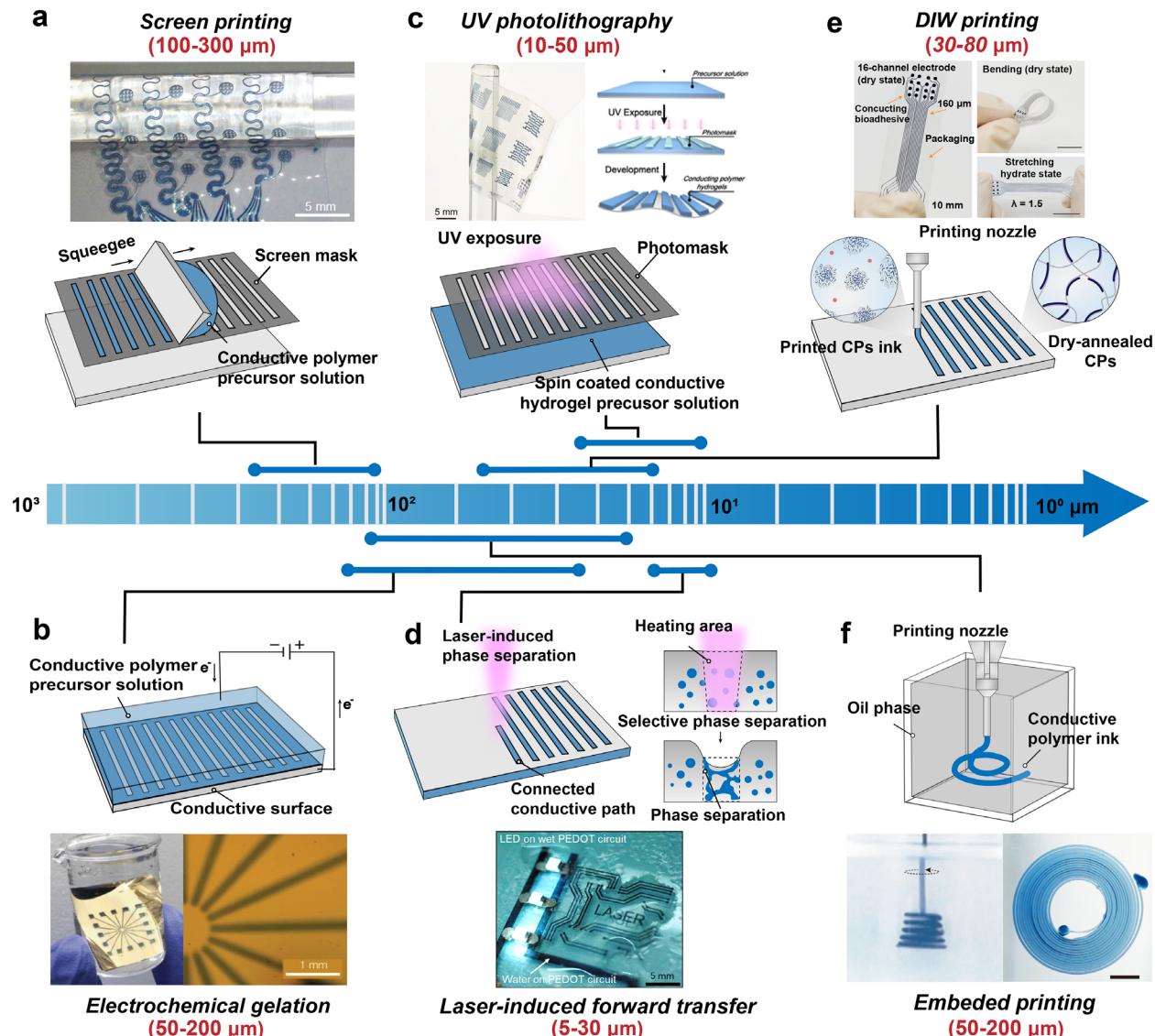


Figure 6. Manufacturing strategies of CPHs-based bioelectronics. Schematic illustration and representative images for those key techniques used for fabricating CPHs-based bioelectronics: a) Screen printing. Reproduced with permission.^[57] Copyright, 2025 AAAS. b) Electrochemical gelation. Reproduced with permission.^[73] Copyright, 2019 Wiley-VCH. c) UV photolithography. Reproduced with permission.^[74] Copyright, 2025 Wiley-VCH. d) Laser-induced forward transfer. Reproduced with permission.^[75] Copyright, 2022 AAAS. e) 3D printing. Reproduced with permission.^[32] Copyright, 2024 Wiley-VCH. f) Liquid-in-liquid printing. Reproduced with permission.^[76] Copyright, 2023 Springer Nature.

detoxification procedures. The significant enhancement in manufacturing precision enables the use of CPHs-based electrodes for precise electrophysiological recording and/or electrical modulation in intricate biological tissues.

In contrast to planar techniques, 3D printing allows the construction of CPHs-based bioelectronics with intricate 3D architectures.^[77] This process employs a layer-by-layer deposition strategy, enabling precise customization for a broad spectrum of applications (Figure 6e).^[32,78] Central to this capability is the development of CPHs inks with tailored rheology. Liu et al. pioneered direct ink writing (DIW)-compatible PEDOT:PSS hydrogels exhibiting shear-thinning behavior and rapid post-extrusion recovery, achieving 80 μm printing resolution through optimized viscoelastic stress-yielding properties.^[32] These inks retain struc-

tural fidelity during extrusion, enabling fabrication of multifunctional systems such as 16-channel all-hydrogel electrode arrays. Demonstrated in rat cardiac electrophysiology, these printed arrays captured spatiotemporal signal dynamics via conformal epicardial interfacing, validating 3D-printed CPHs as a scalable platform for precision bioelectronics.

Liquid-in-liquid 3D printing, a burgeoning technique for crafting soft materials with intricate designs, involves extruding an ink phase into a bath phase as a translational stage follows a 3D design (Figure 6f).^[79,80] Unlike embedded extrusion 3D printing, which necessitates bath phases with unique rheological properties such as shear-thinning or solid-fluid transitions for stability, a novel liquid-in-liquid printing method employs self-assembly, jamming, and coacervation to maintain filament integrity.^[80,81]

Table 1. Comprehensive comparison of various fabrication methods for CPHs.

Methods	Advantages	Disadvantages	Refs.
Screen printing	<ul style="list-style-type: none"> • Cost-efficiency • Pattern customization • Substrate versatility • Material adaptability 	<ul style="list-style-type: none"> • Limited resolution • Rheological constraints • Post-processing challenges (e.g., drying, crosslinking, multilayer alignment) 	[71, 82, 83, 84, 85, 86]
Electrochemical polymerization	<ul style="list-style-type: none"> • High precision (thickness, polymerization rate) • In situ polymerization • eliminating transfer steps 	<ul style="list-style-type: none"> • Complex equipment and process • Material restricted to electroactive monomers • Structural heterogeneity 	[73, 87, 88]
Photolithography	<ul style="list-style-type: none"> • Ultra-high resolution (nanoscale precision) • Controllability and reproducibility • Substrate versatility 	<ul style="list-style-type: none"> • High cost • Multi-step process • Material compatibility challenges (necessitating tailored photosensitive formulations) 	[38, 74, 89]
Laser-assisted patterning	<ul style="list-style-type: none"> • High resolution and precision • Rapid prototyping • Local functionalization 	<ul style="list-style-type: none"> • Thermal damage risk • Material limitations 	[90, 91]
3D printing	<ul style="list-style-type: none"> • Design flexibility and customization • Multi-material integration • High material efficiency • Versatile printing techniques 	<ul style="list-style-type: none"> • Limitation of resolution • Multi-material integration defects • Trade-off between resolution and speed 	[32, 77]

This innovative approach significantly reduces the dependency on rheological properties for both the ink and bath phases. For instance, the interfacial assembly of PEDOT:PSS in an oil-phase solution of the primary amine-terminated surfactant PDMS-NH₂ is likely driven by electrostatic interactions between the sulfonate groups (R-SO₃⁻) of the particle's PSS-rich shell and the protonated amino groups (PDMS-NH₃⁺) from the oil phase, which results in the formation of a stable hydrogel structure.^[76] Despite the significant progress driven by these advanced manufacturing methods, there might be still some certain limitations remain, as detailed in **Table 1**, where future effort could be devoted.

4. Seamless Interfaces between CPHs-Based Electronics and Biological Systems

4.1. CPHs-Tissue Biointerface

Achieving seamless interfacing between CPHs-based electronic devices and biological systems is essential for high-fidelity electrophysiological recording and efficient stimulation (**Figure 7a**).^[10, 15, 92] The ultra-thin and soft CPHs-based electrodes can achieve conformal contact with the complex, curvilinear surfaces of human skin (**Figure 7b**).^[42, 93] However, the dynamic nature of biological tissues, such as the heart and gut, poses extra difficulty for achieving the robust CPHs-tissue interface. While suturing provides a reliable means to affix CPHs-based bioelectronic devices onto tissues or organs, the invasive essence of this method, involving needle penetration and knotting, may induce adverse outcomes including necrosis and infection.^[94] Although these methods facilitate the formation of conformable interface with biological tissues, the stability of these non-covalent interaction on dynamic tissue surfaces remains a grand challenge.^[2, 14]

Chemical adhesion is a promising strategy for non-invasive anchorage of bioelectronic devices.^[94, 95] Hydrogels made of natural polymers like collagen and gelatin offering a plethora of functional groups such as amino, hydroxyl, and carboxyl groups, which are suitable for bioadhesion.^[96] Inspired by the catecholic cross-linking chemistry of 3,4-dihydroxyphenylalanine (DOPA), extensive researches have been conducted to engineer catechol hydrogel-based bioadhesives.^[97] These adhesives benefit from catechol's ability to form strong hydrogen bonds and cation- π interactions, thus enhancing the bioadhesion performance.^[97] The oxidation of catechol to quinone in aerobic, alkaline conditions enables covalent bonding with tissue nucleophiles, making catechol-based adhesives ideal for epidermal electronics.^[97] However, the insufficient adhesion of existing catechol-based hydrogels to moist tissues, with an interfacial toughness below 50 J m⁻²,^[98] is inadequate for establishing a stable and seamless interface. A key reason for the poor interfacial adhesion stability between these CPHs and hydrated biological tissues is the presence of free water at the interface, which hinders the formation of interactive forces between them.^[99] Consequently, rapid removal of interfacial water is critical for establishing robust biointerfaces. An adhesive approach capable of extracting water from the tissue surface prior to forming strong chemical bonds holds significant promise for achieving durable biointegration. Zhao et al. reported a bioadhesion strategy based on dry cross-linking, wherein the polymer dry film drained interfacial water upon contact with wet biological tissues, leading to the formation of a strong biointerface through synergistic hydrogen bonding and chemical anchorage.^[99] Unlike traditional liquid or wet hydrogel-based adhesives that rely on slow (>1 min) diffusion of monomers, macromers, or polymer chains, this method enables the formation of mechanically robust interfaces (>500 J m⁻²)

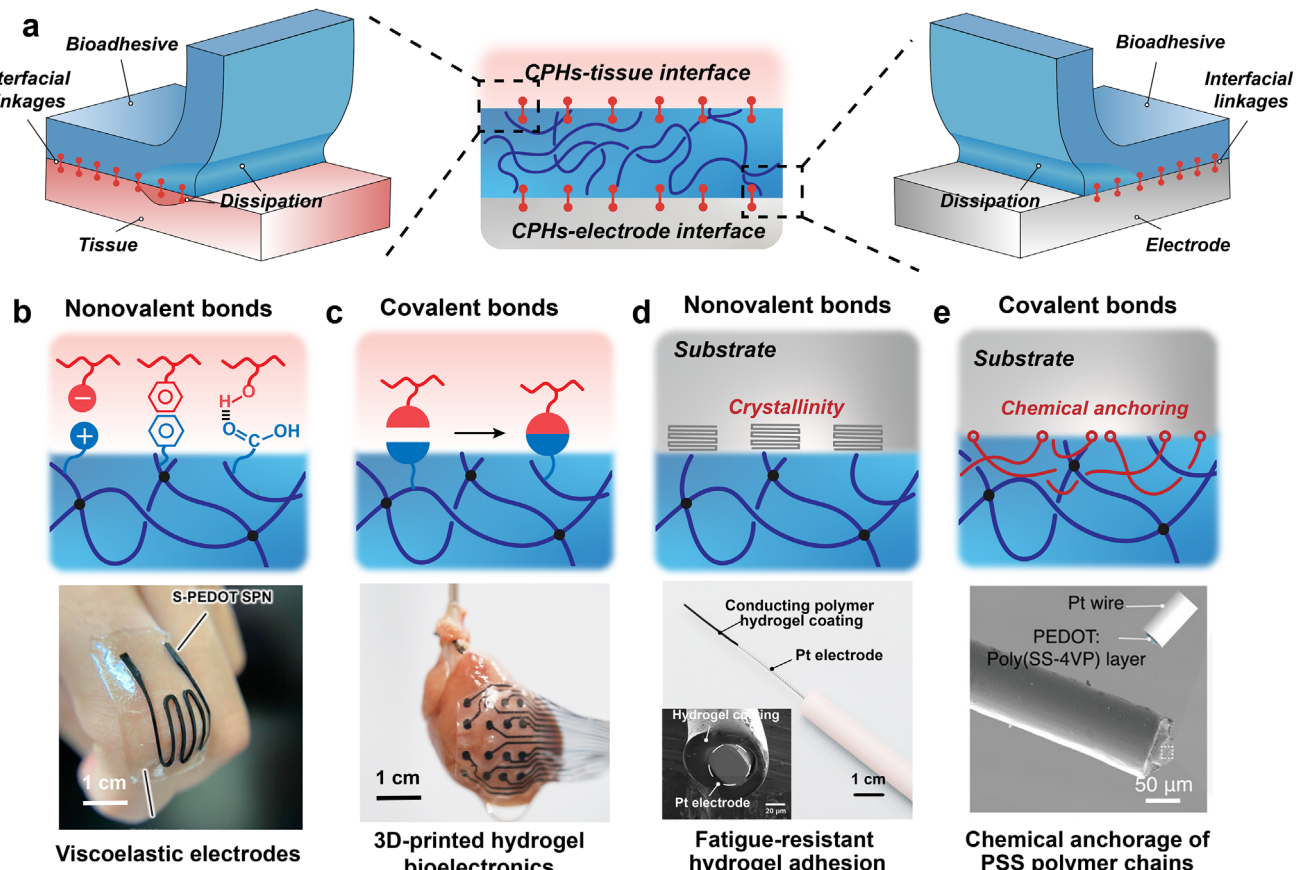


Figure 7. Seamless interfaces between CPHs-based electronics and biological systems. a) Schematic illustration of establishing robust interface between the CPHs and biological tissues, as well as interface between the CPHs and the engineering solids (i.e., metallic electrodes). b,c) Interfacial adhesion between CPHs and biological tissues is formed through interfacial covalent (i.e., amide group, b) and/or noncovalent bonds (i.e., hydrogen bonds, electrostatic interaction, c). b) Reproduced with permission from ref. [42] Copyright 2023 Wiley-VCH. c) Reproduced with permission from ref. [47] Copyright 2023 Wiley-VCH. d,e) Interfacial adhesion between CPHs and engineering solids is formed through chemical anchorage of long-chain polymers (d), noncovalent interactions, and/or mechanical interlock (e). d) Reproduced with permission from ref. [31] Copyright 2023 Wiley-VCH. e) Reproduced with permission from ref. [67] Copyright 2023 Wiley-VCH.

within seconds (< 5 s). The entanglement of long-chain polymers acts as energy dissipation components, contributing to the toughness of the interface. Leveraging this bioadhesion technology, various hydrogel materials are firmly anchored onto various wet and dynamic biological tissues.

To enhance the electrical properties and bioadhesive capabilities of CPHs, Liu et al. incorporated CPs (e.g., PEDOT:PSS) alongside bioadhesive moieties (e.g., PAA-NHS) within the hydrogel network, complemented by biocompatible polymers such as chitosan (CTS) and PVA to form the hydrogel precursor (Figure 7c).^[32] The amidation reaction between PAA-NHS and CTS, combined with hydrogen bonding among these polymer chains, synergistically contributed to forming a tough, interconnected network. Additionally, utilizing the dry cross-linking mechanism enabled CPHs-based bioelectrodes to establish mechanically conformal interfaces with various tissues, with an interfacial toughness of ≈ 200 J m $^{-2}$. Such adhesion maintains long-term stability even under vigorous body movements. Furthermore, these CPHs exhibit a high CSC of 5.83 mC cm $^{-2}$ and a low modulus of 650 kPa, rendering them both mechanically compliant and electrochemically suitable for bioelectronic interfaces.

However, the strong adhesion poses challenges for benign device removal, as forceful detachment risks tissue damage or inflammation. To address this, prior work demonstrated that incorporating stimuli-responsive bonds (e.g., boronate-diol complexes) enables on-demand interfacial weakening (from 400 to 40 J m $^{-2}$) upon exposure to biocompatible triggers like glucose, allowing safe device retrieval without residual harm.^[43] These advances highlight the potential of chemically engineered CPHs to reconcile robust bioelectronic interfacing with clinical safety requirements.

4.2. CPHs-Solid Substrate Interface

The secure attachment of CPHs to solid electrodes is essential for ensuring the effectiveness and durability of bioelectronic devices. A primary failure mechanism, however, stems from the cyclic volumetric changes of the CPH during repeated charge injection and ejection. This mechanical stress inevitably leads to fatigue crack propagation and interfacial delamination, which progressively degrades the electrode-tissue interface and ultimately

culminates in complete device failure.^[67,90,100] To address this challenge, Liu et al. developed a PEDOT:PSS/PVA hydrogel coating on metallic electrodes via a dip-coating method, followed by air-drying and thermal annealing. This process promotes the formation of ordered nanocrystalline domains at the CPHs-electrode interface (Figure 7d). The interfacial fatigue threshold of this CPHs coating reached as high as 330 J m^{-2} , which is over two orders of magnitude higher than that of spin-coated PEDOT:PSS ($\approx 2 \text{ J m}^{-2}$).^[31] This fabrication approach not only offers a practical route for creating durable and robust bioelectronic interfaces but also effectively addresses the longstanding issue of coating longevity.

However, the incorporation of insulating PVA resulted in relatively low electrical conductivity ($\approx 9 \text{ S m}^{-1}$), potentially compromising the efficacy of electrophysiological recording and stimulation. To simultaneously enhance interfacial stability and conductivity, we recently developed CPHs with an IPN structure. This involved chemically anchoring a functional long-chain polymer, poly(styrene sulfonate-*co*-4-vinyl pyridine) (Poly(SS-4VP)), onto a metallic substrate, followed by electrochemical deposition of PEDOT, and subsequent chemical crosslinking of the Poly(SS-4VP) chains (Figure 7e).^[67] The resulting 130-nm-thick PEDOT:Poly(SS-4VP) hydrogel coating exhibited a Young's modulus of $\approx 800 \text{ kPa}$ in the hydrated state, indicating excellent mechanical compliance. Importantly, these CPHs demonstrated not only superior electrochemical performance but also markedly improved electrochemical stability, with only $\approx 9\%$ reduction in CSC after 10000 charge-discharge cycles. More recently, Ko et al. demonstrated a strategy that combines laser-induced phase separation with interfacial structural engineering to achieve strong adhesion of PEDOT:PSS hydrogels onto polymer substrates.^[90] Laser irradiation of the PEDOT:PSS film induces its phase separation and simultaneously promotes the formation of a nanoscale, interlocked structure at the interface with the substrate. CPHs-based bioelectronics fabricated via this technique maintained excellent electrochemical properties even after 8 months of storage in a physiological environment. This stability meets the criteria necessary for long-term electrical stimulation and electrophysiological recording.

5. CPHs-Based Electronic for High-Performance Biointerfacing

CPHs interfaces, with their tissue-like mechanical attributes, ionic-electronic conductivity, and excellent biocompatibility, are poised to revolutionize the bioelectronics in recording, stimulation, and biosensing. These CPHs-based bioelectronics seamlessly interface with human physiology to enable real-time monitoring of electrophysiological signals and physiological parameters, and they also promote tissue recovery and modulate organ functions through electrical intervention (Figure 8). These CPHs-based bioelectronics offer distinct advantages over traditional electronics based on metal/silicon materials, such as improved long-term stability and reduced risk of tissue damage, facilitating seamless integration and enhancing the device performance. In this section, we will present an overview on the application of CPHs interfaces in wearable and implantable bioelectronics, and also underscore their substantial contributions to fields

such as electrophysiological recording, electrical stimulation, and biosensing.

5.1. Electrophysiological Recording

Electrophysiological recording is essential for interpreting physiological activities, providing diagnostic and therapeutic insights into biological systemic functions.^[14,101] Bioelectrical signals include electroencephalography (EEG), electrocorticography (ECoG), electrocardiography (ECG), epicardial ECG (eECG), and electromyography (EMG) have been recorded clinically.^[7,102] The principal challenge in electrophysiological recording is achieving a high SNR, which is contingent on the transduction efficiency of ion concentration fluctuations at the tissue-electrode interface.^[28] The seamless interface of CPHs with tissue, along with their hybrid ion- and electron conduction mode, contributes to reduced impedance and enhanced electrophysiological recording capabilities. Moreover, the tissue-like mechanics and favorable biocompatibility of CPHs can mitigate foreign body and inflammatory reactions, thereby enhancing signal quality and reliability for prolonged periods.^[10]

The skin, serving as the body's expansive gateway to the external environment, offers a critical platform for extracting physical and chemical biomarker information.^[1,103] In epidermal bioelectronics, also known as *e*-skin, contact impedance refers to the complex impedance encountered at the electrode-skin interface during signal acquisition.^[103] Elevated contact impedance can lead to voltage attenuation, reduced signal amplitude, and increased noise, thus deteriorating the SNR and data quality.^[11,14,101] Although the CPHs interface offers a distinct advantage in reducing interfacial contact impedance, signal quality is still susceptible to interference from motion artifacts.^[4] CPHs equipped with bioadhesive capabilities ensure a secure and steadfast bond with the skin, effectively reducing motion-induced artifacts by maintaining stable interfacial impedance during physical activity, thereby preserving high-quality signal integrity.^[39] For instance, a CPH composed of PEDOT and PDA achieved strong adhesion to the skin (shear strength $\approx 20 \text{ kPa}$), enabling high-fidelity eECG recording during motion that maintained a SNR of $\approx 12 \text{ dB}$, consistent with the value at rest.^[51] Furthermore, CPHs with strain-insensitive characteristics can minimize impedance fluctuations resulting from tissue deformation, ensuring stable and reliable electrophysiological measurements. By employing a bicontinuous structure of PVA-polyvinylpyrrolidone and PEDOT:PSS, the CPHs retain their conductivity at 50% strain, effectively eliminating motion artifacts from arm swinging in EMG recordings.^[58]

Unlike wearable electronics, implantable electronics are invasive and directly integrated with the tissues or organs of a living organism.^[2] The integration enables unprecedented spatiotemporal resolution, facilitating precise and real-time monitoring of electrophysiological activities.^[13] By circumventing the signal-attenuating and noise-inducing barriers of the skin and subcutaneous tissues, implantable systems facilitate the precise, real-time monitoring of fast electrophysiological activities, such as neuronal action potentials or cardiac arrhythmias, which are critical for understanding fundamental biological processes and diagnosing pathological conditions.^[7] However, the chronic failure of

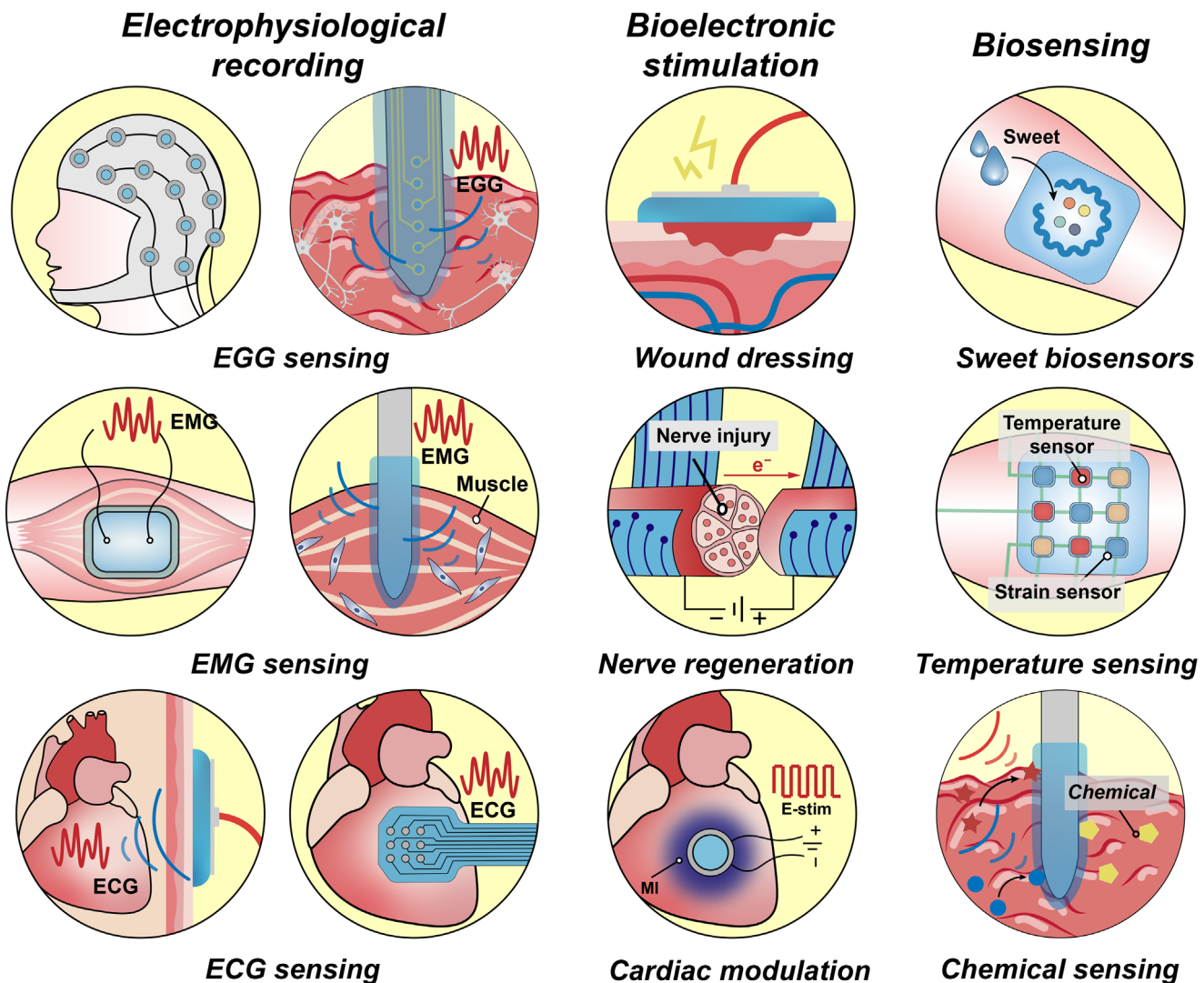


Figure 8. Various examples of CPH-based bioelectronics for wearable and implantable applications around the living organisms. CPH-based bioelectronics interact with the human body to facilitate continuous monitoring of electrophysiological signals (e.g., EGG, EMG, ECG) and physiological parameters (e.g., sweet components, temperature, and various biomarkers), while also promoting tissue repair (e.g., skin healing, nerve regeneration) and regulating organ functions (e.g., heart rate, neurotransmission) through electrical stimulation.

rigid implants stems from an unavoidable mechanical mismatch with the host tissue, which initiates a foreign body response that insulates the electrode and degrades signal quality over time, thus presenting the significant challenge for their long-term clinical viability.^[101,104] The application of a soft CPHs coating onto metal electrodes has been demonstrated to effectively mitigate these risks while concurrently enhancing signal quality.^[7] This favorable interaction effectively mitigates the severity of the FBR, minimizing fibrotic encapsulation and promoting a more stable and biocompatible interface.^[104] Furthermore, the inherent ionic-electronic conductivity of CPHs enhances charge transfer capabilities, thereby improving signal quality and lowering the electrochemical impedance. The high-fidelity electrophysiological monitoring in the dorsal hippocampus of rat models has sustained reliable recordings for over four weeks, with impedance values consistently remaining below 250 k Ω (1 kHz) throughout

the duration.^[67] To address the challenge of interfacing with dynamic organs like the heart, we developed an all-hydrogel bioelectronic device that establishes robust adhesion to moving tissues. This adhesive design yields a substantially higher SNR of ≈ 40 , vastly outperforming non-adhesive hydrogel devices (SNR ≈ 2).^[32] The resulting stable, high-fidelity signal acquisition, facilitated by a compliant and adhesive interface, is critical for achieving long-term, high-precision spatiotemporal monitoring of epicardial activity and represents a significant leap toward the clinical translation of chronic implants.

5.2. Bioelectronic Stimulation

Bioelectronic stimulation, a cornerstone technique in bioelectronics, involves the strategic application of controlled

electrical currents to biological tissues to modulate physiological processes.^[29] As a non-pharmacological intervention, it is extensively employed in clinical settings to address various medical disorders by targeting neural and muscular pathways.^[29,101] Conventional dry and rigid electrodes, however, are prone to mechanical misalignment, precluding the delivery of consistent and reliable electrical stimulation required for precise therapeutic interventions.^[10] A soft, low-impedance, adhesive CPHs electrodes can provide a stable and compliant interface essential for effective signal transmission and energy delivery.^[105,106] The superior conformability of CPHs to the wound surface, coupled with their excellent electrical attributes, markedly improves the efficacy of biomedical devices by reducing movement disturbance and optimizing electrical connectivity. For instance, Bao et al. engineered a CPH-based smart bandage capable of on-demand skin adhesion, continuous physiological monitoring, and targeted electrical stimulation, which collectively accelerated wound closure, promoted neovascularization, and enhanced dermal recovery.^[105] Consequently, the use of CPHs as an interface significantly accelerates wound healing, promotes neovascularization, and enhances dermal regeneration, highlighting the pivotal role of CPHs in electrotherapeutic wound repair.^[107]

Electrical stimulation technology has also been applied in more invasive scenarios, such as cardiac pacemakers, deep brain stimulators, and neural electrodes.^[29] As with other *in vivo* applications, electrodes used for electrical stimulation should have mechanical properties that match those of biological tissues to prevent inflammatory responses and fibrous encapsulation due to modulus mismatches. Moreover, for safe and effective bioelectrical stimulation, it is crucial to elicit excitation in excitable cells without causing over-stimulation or collateral damage.^[29] This necessitates the use of lower stimulation voltages to achieve optimal electrical activation. However, metal electrodes generally possess a low *CIC* ($< 1 \text{ mC cm}^{-2}$), which hampers the delivery of significant charge at low voltages necessary to well-executed electrical stimulation. Liu et al. has demonstrated that a CPHs coating not only establishes a mechanically compatible interface for tissue interaction but also significantly enhances the electrode's *CIC* up to 4.4 mC cm^{-2} . The CPHs coating significantly reduces the pacing threshold voltage for cardiac stimulation to 0.7 V, compared to $\approx 2.0 \text{ V}$ for metal electrodes, thereby emphasizing the pivotal role of CPHs in enabling low-voltage stimulation.^[31] Impedance matching at bioelectronic interfaces is critical beyond mechanical compatibility, as elevated interfacial impedance increases reliance on higher stimulation voltages and charge densities, heightening risks of tissue damage and off-target physiological effects (e.g., arrhythmias from current dispersion). CPHs address this challenge through nanostructure-enhanced charge transfer kinetics and expanded electrochemically active surface areas, enabling efficient stimulation at reduced voltages. Shan et al. demonstrated this principle via 3D-printed hydrogel bioelectronics that transition from planar 2D constructs to self-curling nerve interfaces upon hydration, achieving an interfacial impedance of $\approx 150 \Omega$ at 1 kHz.^[108] This seamless integration permits ultralow-voltage neural activation ($\approx 10 \text{ mV}$), as validated in vagus nerve stimulation for post-stroke recovery, where the system enhanced cerebral blood flow, reduced infarct size, and accelerated motor rehabilitation by maintaining targeted bioelectronic coupling without collateral excitation.

5.3. Biosensing

In addition to electrically related physical signals, the human body conveys a range of physiological information through metrics such as pressure, temperature, and pH, which collectively indicate its basic physiological condition.^[1,9] Due to its tissue-like softness, strain sensitivity, and environmental adaptability, CPHs is considered as an ideal platform for monitoring tissue movement and deformation.^[53] When subjected to strain, the internal resistance of the CPHs undergoes alterations, functioning as an effective method for sensing and tracking variations in tissue strain/pressure.^[109] The potential of this sensor is further demonstrated by its integration with electronic skins for measuring diverse physiological signals and recognizing hand gestures, highlighting its versatile application in wearable technology.

Additionally, fluctuations in temperature or pH can also alter the resistance of CPHs, endowing them with the capability to monitor these physiological signals. For CPHs-based temperature sensors, long-term stability is paramount, as hydrogels are susceptible to dehydration in high-temperature environments, compromising their electrical and mechanical integrity. As a result, it is often necessary to incorporate high-boiling-point hydrophilic solvents, hydratable salts, or employ precise encapsulation techniques to maintain water content stability.^[110] Additionally, the electrical properties of most CPs, such as PANi, undergo significant changes across various pH levels. This behavior results from pH-induced adjustments to the doping level within the polymer matrix, enabling these materials to function as pH sensors. However, it is observed that the impedance of the majority of CPHs undergoes a marked increase in response to an elevation in pH levels, which could impair the efficacy of the sensors. A homogeneously conducting CPHs made from PEDOT:PSS and PANi displays low impedance across the entire frequency range, with the impedance increasing from 23.7 to 157 ohms as the pH rises from 1 to 7, yet it still meets the criteria for high-fidelity electric transmission.^[39] This CPHs-based pH sensor to monitor gastrointestinal fluids, where it reliably detected a potential of 229.5 mV, corresponding to the electrochemical profile of a pH 2 buffer. This confirmed the sensor's precise pH measurement capability.

Chemical sensing for human physiological monitoring offers accurate and real-time monitoring of biomarkers, delivering immediate health assessments and facilitating early disease detection.^[111] This technology enhances personalized healthcare by continuously tracking biomarker fluctuations, improving patient management and outcomes. Achieving high sensitivity and selectivity in chemical sensors necessitates integrating biological recognition elements (e.g., enzymes, antibodies, DNA) with electronic mediators to optimize signal transduction.^[9] Traditional dry electrodes encounter significant challenges in terms of loading sufficient quantities of biological recognition elements and ensuring effective electronic communication between these elements and the corresponding electronic mediators. The 3D polymer network of CPHs provides ample space for the immobilization of biological elements, and the high electroactivity of CPs facilitates efficient electron transfer, thereby enhancing the sensing performance of CPHs-based biosensors. Efficient sweat capture is crucial for non-invasive sweat sensing, yet it is hindered by the challenge of accessing biofluids. Utilizing an ionic

conducting hydrogel as an ionic conduction pathway for biomarkers facilitates solvation and diffusion of solid-state biomarkers. This sensor is capable of monitoring water-insoluble analytes, such as solid cholesterol, with ultralow detection limits reaching $0.26 \text{ nmol cm}^{-2}$, and it can continuously track postprandial changes in cholesterol concentration in individuals.^[71]

6. Summary and Perspectives

This review summarizes recent advances in CPHs-based bioelectronic interfacing technologies. Specifically, we focus on the physical, chemical, and biological properties of CPHs, the design principles underpinning high-performance materials, and innovative processing and manufacturing strategies for CPHs-based electronics. Various healthcare-related applications leveraging CPHs-based bioelectronic interfaces are discussed, including wearable and implantable devices for electrophysiological signal recording, biosensing, electrical stimulation, and theranostic platforms. The discussion also critically evaluates current limitations in material design, manufacturing scalability, and clinical translation, providing a roadmap for future developments in bioelectronic interfaces.

- 1) **Material Design.** Despite significant advancements in optimizing individual properties of CPHs, critical trade-offs persist. The complex biological environment demands the development of innovative materials capable of integrating multiple desirable properties: mechanical robustness (including strength, toughness, and fatigue resistance), stable electrical conductivity, durable yet reversible interfacial adhesion, and biocompatibility. Achieving seamless integration of these attributes is essential for advancing soft bioelectronics and enabling next-generation implantable and wearable devices that interact effectively with biological tissues. Additionally, while CPHs are vital for bridging electronics and biology, they often lack intrinsic cellular functionalities necessary for tissue regulation. As such, current CPHs-based bioelectronics, especially those aimed at inflammation monitoring, are limited in their capacity to modulate immune responses. Enhancing their biomedical utility requires interfaces with bioactivity tailored to cellular signaling mechanisms (e.g., bacterial or mammalian pathways) to enable inflammation control and tissue regeneration.
- 2) **Processing and Manufacturing.** Advancing the fabrication of CPHs-based bioelectronics is crucial to meet the demand for miniaturized, high-performance implantable devices. Scalability remains a major challenge, necessitating production protocols that maintain precision and quality at larger volumes. A promising approach involves integrating AI-driven optimization and predictive modeling into manufacturing workflows to improve precision, efficiency, and scalability. Such strategies could accelerate breakthroughs in device miniaturization, performance, and manufacturability, democratizing access to cutting-edge medical technologies.
- 3) **Biomedical Applications.** While CPHs-based bioelectronics have made strides, their inability to perform comprehensive multimodal monitoring and therapeutic intervention limits their versatility in treating complex diseases. To address this, future platforms must integrate multiple func-

tional electrodes within a single CPHs system, enabling real-time, high-precision electrophysiological recording, biosensing, and stimulation. Expanding these multimodal capabilities will pave the way for personalized, adaptive therapies, transforming biomedical technologies and improving clinical outcomes.

Acknowledgements

Y.X. and Z.N. contributed equally to this work. The authors acknowledge the financial support by the STI 2030-Major Projects (2022ZD0209500), the National Natural Science Foundation of China (52373139, U2436202 and 52503156), the Basic Research Program of Shenzhen (JCYJ20230807093419041, JCYJ20240813094159001, and 20231116101626002). The authors also gratefully acknowledge the support from the Shenzhen Science and Technology Innovation Commission (KJZD20240903101400001) and the Development and Reform Commission of Shenzhen Municipality (XMHT20240115003).

Conflict of Interest

The authors declare no conflict of interest.

Keywords

bioelectronics, biointerfacing, bioadhesion, conducting polymer hydrogels, engineering

Received: August 14, 2025
Revised: November 13, 2025
Published online:

- [1] C. Zhao, J. Park, S. E. Root, Z. Bao, *Nat. Rev. Bioeng.* **2024**, 2, 671.
- [2] R. Feiner, T. Dvir, *Nat. Rev. Mater.* **2017**, 3, 17076.
- [3] S. Oh, J. Jekal, J. Liu, J. Kim, J.-U. Park, T. Lee, K.-I. Jang, *Adv. Funct. Mater.* **2024**, 34, 2403562.
- [4] J. Yin, S. Wang, T. Tat, J. Chen, *Nat. Rev. Bioeng.* **2024**, 2, 541.
- [5] D. Kireev, S. Kutagullu, J. Hong, M. N. Wilson, M. Ramezani, D. Kuzum, J.-H. Ahn, D. Akinwande, *Nat. Rev. Mater.* **2024**, 9, 906.
- [6] Q. Zheng, Q. Tang, Z. L. Wang, Z. Li, *Nat. Rev. Cardiol.* **2021**, 18, 7.
- [7] Z. Zhang, Z. Zhu, P. Zhou, Y. Zou, J. Yang, H. Haick, Y. Wang, *ACS Nano* **2023**, 17, 17634.
- [8] Z. Liu, Y. Hu, X. Qu, Y. Liu, S. Cheng, Z. Zhang, Y. Shan, R. Luo, S. Weng, H. Li, H. Niu, M. Gu, Y. Yao, B. Shi, N. Wang, W. Hua, Z. Li, Z. L. Wang, *Nat. Commun.* **2024**, 15, 507.
- [9] P. Zhang, B. Zhu, P. Du, J. Travas-Sejdic, *Chem. Rev.* **2024**, 124, 722.
- [10] H. Yuk, J. Wu, X. Zhao, *Nat. Rev. Mater.* **2022**, 7, 935.
- [11] X. Liu, J. Liu, S. Lin, X. Zhao, *Mater. Today* **2020**, 36, 102.
- [12] A. P. Liu, E. A. Appel, P. D. Ashby, B. M. Baker, E. Franco, L. Gu, K. Haynes, N. S. Joshi, A. M. Kloxin, P. H. J. Kouwer, J. Mittal, L. Morsut, V. Noireaux, S. Parekh, R. Schulman, S. K. Y. Tang, M. T. Valentine, S. L. Vega, W. Weber, N. Stephanopoulos, O. Chaudhuri, *Nat. Mater.* **2022**, 21, 390.
- [13] Y. Li, N. Li, N. De Oliveira, S. Wang, *Matter* **2021**, 4, 1125.
- [14] X. Chen, Y. Feng, P. Zhang, Z. Ni, Y. Xue, J. Liu, *Adv. Mater.* **2025**, 37, 2413476.
- [15] Q. Yang, Z. Hu, J. A. Rogers, *Acc. Mater. Res.* **2021**, 2, 1010.
- [16] F. Fu, J. Wang, H. Zeng, J. Yu, *ACS Mater. Lett.* **2020**, 2, 1287.
- [17] T. Zhu, Y. Ni, G. M. Biesold, Y. Cheng, M. Ge, H. Li, J. Huang, Z. Lin, Y. Lai, *Chem. Soc. Rev.* **2023**, 52, 473.

[18] P. Zhang, Y. Yang, Z. Li, Y. Xue, F. Wang, L. Shan, Y. Wang, X. Shi, K. Wu, J. Liu, *Adv. Funct. Mater.* **2025**, *35*, 2422869.

[19] A. Roy, R. Afshari, S. Jain, Y. Zheng, M.-H. Lin, S. Zenkar, J. Yin, J. Chen, N. A. Peppas, N. Annabi, *Chem. Soc. Rev.* **2025**, *54*, 2595.

[20] W. U. Khan, Z. Shen, S. M. Mugo, H. Wang, Q. Zhang, *Chem. Soc. Rev.* **2025**, *54*, 2832.

[21] L. Ding, Z.-D. Yu, X.-Y. Wang, Z.-F. Yao, Y. Lu, C.-Y. Yang, J.-Y. Wang, J. Pei, *Chem. Rev.* **2023**, *123*, 7421.

[22] T. Nezakati, A. Seifalian, A. Tan, A. M. Seifalian, *Chem. Rev.* **2018**, *118*, 6766.

[23] Z. Sun, Q. Ou, C. Dong, J. Zhou, H. Hu, C. Li, Z. Huang, *Exploration* **2024**, *4*, 20220167.

[24] T. Zhou, H. Yuk, F. Hu, J. Wu, F. Tian, H. Roh, Z. Shen, G. Gu, J. Xu, B. Lu, X. Zhao, *Nat. Mater.* **2023**, *22*, 895.

[25] Y. Zhang, Y. Tan, J. Lao, H. Gao, J. Yu, *ACS Nano* **2023**, *17*, 9681.

[26] Y. Liu, R. Omar, G. Li, P. Zhou, Y. Zhang, W. Yan, H. Haick, C. F. Guo, T. Someya, Y. Wang, *Prog. Mater. Sci.* **2025**, *157*, 101590.

[27] P. Zarrintaj, S. Manouchehri, Z. Ahmadi, M. R. Saeb, A. M. Urbanska, D. L. Kaplan, M. Mozafari, *Carbohydr. Polym.* **2018**, *187*, 66.

[28] J. Zhang, Z. Cheng, P. Li, B. Tian, *Nat. Rev. Mater.* **2025**, *10*, 425.

[29] Y. Huang, K. Yao, Q. Zhang, X. Huang, Z. Chen, Y. Zhou, X. Yu, *Chem. Soc. Rev.* **2024**, *53*, 8632.

[30] C. Boehler, S. Carli, L. Fadiga, T. Stieglitz, M. Asplund, *Nat. Protoc.* **2020**, *15*, 3557.

[31] Y. Xue, X. Chen, F. Wang, J. Lin, J. Liu, *Adv. Mater.* **2023**, *35*, 2304095.

[32] F. Wang, Y. Xue, X. Chen, P. Zhang, L. Shan, Q. Duan, J. Xing, Y. Lan, B. Lu, J. Liu, *Adv. Funct. Mater.* **2024**, *34*, 2314471.

[33] M. Yang, P. Chen, X. Qu, F. Zhang, S. Ning, L. Ma, K. Yang, Y. Su, J. Zang, W. Jiang, T. Yu, X. Dong, Z. Luo, *ACS Nano* **2023**, *17*, 885.

[34] X. Huang, C. Chen, X. Ma, T. Zhu, W. Ma, Q. Jin, R. Du, Y. Cai, M. Zhang, D. Kong, M. Wang, J. a. Ren, Q. Zhang, X. Jia, *Adv. Funct. Mater.* **2023**, *33*, 2302846.

[35] S. Zhang, Y. Chen, H. Liu, Z. Wang, H. Ling, C. Wang, J. Ni, B. Çelebi-Saltik, X. Wang, X. Meng, H.-J. Kim, A. Baidya, S. Ahadian, N. Ashammakh, M. R. Dokmeci, J. Travas-Sejdic, A. Khademhosseini, *Adv. Mater.* **2020**, *32*, 1904752.

[36] G. Li, K. Huang, J. Deng, M. Guo, M. Cai, Y. Zhang, C. F. Guo, *Adv. Mater.* **2022**, *34*, 2200261.

[37] B. Lu, H. Yuk, S. Lin, N. Jian, K. Qu, J. Xu, X. Zhao, *Nat. Commun.* **2019**, *10*, 1043.

[38] Y. Liu, J. Liu, S. Chen, T. Lei, Y. Kim, S. Niu, H. Wang, X. Wang, A. M. Foudeh, J. B. H. Tok, Z. Bao, *Nat. Biomed. Eng.* **2019**, *3*, 58.

[39] Y. Shin, H. S. Lee, Y. J. Hong, S.-H. Sunwoo, O. K. Park, S. H. Choi, D.-H. Kim, S. Lee, *Sci. Adv.* **2024**, *10*, adi7724.

[40] J. Chong, C. Sung, K. S. Nam, T. Kang, H. Kim, H. Lee, H. Park, S. Park, J. Kang, *Nat. Commun.* **2023**, *14*, 2206.

[41] B. Yao, Y. Yan, Q. Cui, S. Duan, C. Wang, Y. Du, Y. Zhao, D. Wu, S. Wu, X. Zhu, T. Hsiai, X. He, *Matter* **2022**, *5*, 4407.

[42] S. J. K. O'Neill, M. Ashizawa, A. M. McLean, R. R.-M. Serrano, T. Shimura, M. Agetsuma, M. Tsutsumi, T. Nemoto, C. D. J. Parmenter, J. A. McCune, G. G. Malliaras, N. Matsuhsisa, O. A. Scherman, *Adv. Mater.* **2025**, *37*, 2415687.

[43] E. Song, J. Li, S. M. Won, W. Bai, J. A. Rogers, *Nat. Mater.* **2020**, *19*, 590.

[44] M. N. Gueye, A. Carella, J. Faure-Vincent, R. Demadrille, J.-P. Simonato, *Prog. Mater Sci.* **2020**, *108*, 100616.

[45] Y. Li, Y. Pang, L. Wang, Q. Li, B. Liu, J. Li, S. Liu, Q. Zhao, *Adv. Mater.* **2024**, *36*, 2310973.

[46] W. Li, Y. Li, Z. Song, Y.-X. Wang, W. Hu, *Chem. Soc. Rev.* **2024**, *53*, 10575.

[47] X. Fan, W. Nie, H. Tsai, N. Wang, H. Huang, Y. Cheng, R. Wen, L. Ma, F. Yan, Y. Xia, *Adv. Sci.* **2019**, *6*, 1900813.

[48] C. F. Guimarães, L. Gasperini, A. P. Marques, R. L. Reis, *Nat. Rev. Mater.* **2020**, *5*, 351.

[49] S. Wang, Y. Nie, H. Zhu, Y. Xu, S. Cao, J. Zhang, Y. Li, J. Wang, X. Ning, D. Kong, *Sci. Adv.* **2022**, *8*, abl5511.

[50] S. Yang, X. Jiang, *ACS Nano* **2024**, *18*, 27107.

[51] J. Lao, Y. Jiao, Y. Zhang, H. Xu, Y. Wang, Y. Ma, X. Feng, J. Yu, *ACS Nano* **2025**, *19*, 7755.

[52] X. He, D. Liu, B. Cui, H. Huang, S. Dai, I. Pang, Y. Qiao, T. Xu, S. Zhang, *Adv. Funct. Mater.* **2024**, *34*, 2405896.

[53] Z. Zhang, G. Chen, Y. Xue, Q. Duan, X. Liang, T. Lin, Z. Wu, Y. Tan, Q. Zhao, W. Zheng, L. Wang, F. Wang, X. Luo, J. Xu, J. Liu, B. Lu, *Adv. Funct. Mater.* **2023**, *33*, 2305705.

[54] X. Zhao, X. Chen, H. Yuk, S. Lin, X. Liu, G. Parada, *Chem. Rev.* **2021**, *121*, 4309.

[55] J. Lou, D. J. Mooney, *Nat. Rev. Chem.* **2022**, *6*, 726.

[56] H. Montazerian, E. Davoodi, C. Wang, F. Lorestani, J. Li, R. Haghniaz, R. R. Sampath, N. Mohaghegh, S. Khorasvi, F. Zehtabi, Y. Zhao, N. Hosseinzadeh, T. Liu, T. K. Hsiai, A. H. Najafabadi, R. Langer, D. G. Anderson, P. S. Weiss, A. Khademhosseini, W. Gao, *Nat. Commun.* **2025**, *16*, 3755.

[57] M. S. Rahman, A. Shon, R. Joseph, A. Pavlov, A. Stefanov, M. Namkoong, H. Guo, D. Bui, R. Master, A. Sharma, J. Lee, M. Rivas, A. Elati, Y. Jones-Hall, F. Zhao, H. Park, M. A. Hook, L. Tian, *Sci. Adv.* **2025**, *11*, ads4415.

[58] Q. Han, X. Gao, C. Zhang, Y. Tian, S. Liang, X. Li, Y. Jing, M. Zhang, A. Wang, S. Bai, *Advanced Materials* **2025**, *37*, 2415445.

[59] R. A. Nasser, S. S. Arya, K. H. Alshehhi, J. C. M. Teo, C. Pitsalidis, *Trends Biotechnol.* **2024**, *42*, 760.

[60] S. Zhang, H. Fang, H. Tian, *Biomacromolecules* **2024**, *25*, 7015.

[61] W.-L. Lei, C.-W. Peng, S.-C. Chiu, H.-E. Lu, C.-W. Wu, T.-Y. Cheng, W.-C. Huang, *Adv. Funct. Mater.* **2024**, *34*, 2307365.

[62] J. Tropp, C. P. Collins, X. Xie, R. E. Daso, A. S. Mehta, S. P. Patel, M. M. Reddy, S. E. Levin, C. Sun, J. Rivnay, *Adv. Mater.* **2024**, *36*, 2306691.

[63] X. Li, J. P. Gong, *Nat. Rev. Mater.* **2024**, *9*, 380.

[64] V. R. Feig, H. Tran, M. Lee, Z. Bao, *Nat. Commun.* **2018**, *9*, 2740.

[65] H. Wei, M. Lei, P. Zhang, J. Leng, Z. Zheng, Y. Yu, *Nat. Commun.* **2021**, *12*, 2082.

[66] L. Li, Y. Zhang, H. Lu, Y. Wang, J. Xu, J. Zhu, C. Zhang, T. Liu, *Nat. Commun.* **2020**, *11*, 62.

[67] J. Zhang, L. Wang, Y. Xue, I. M. Lei, X. Chen, P. Zhang, C. Cai, X. Liang, Y. Lu, J. Liu, *Adv. Mater.* **2023**, *35*, 2209324.

[68] S. Duan, M. Hua, C. W. Zhang, W. Hong, Y. Yan, A. Jazza, C. Chen, P. Shi, M. Si, D. Wu, Z. Lin, P. He, Y. Du, X. He, *Chem. Rev.* **2025**, *125*, 7918.

[69] T. Yang, C. Xu, C. Liu, Y. Ye, Z. Sun, B. Wang, Z. Luo, *Chem. Eng. J.* **2022**, *429*, 132430.

[70] R. Wang, Y. Peng, C. Liu, D. Zheng, J. Yu, *J. Colloid Interface Sci.* **2024**, *673*, 143.

[71] R. T. Arwani, S. C. L. Tan, A. Sundarapandi, W. P. Goh, Y. Liu, F. Y. Leong, W. Yang, X. T. Zheng, Y. Yu, C. Jiang, Y. C. Ang, L. Kong, S. L. Teo, P. Chen, X. Su, H. Li, Z. Liu, X. Chen, L. Yang, Y. Liu, *Nat. Mater.* **2024**, *23*, 1115.

[72] P. Andersson Ersman, R. Lassnig, J. Strandberg, D. Tu, V. Keshmiri, R. Forchheimer, S. Fabiano, G. Gustafsson, M. Berggren, *Nat. Commun.* **2019**, *10*, 5053.

[73] V. R. Feig, H. Tran, M. Lee, K. Liu, Z. Huang, L. Beker, D. G. Mackanic, Z. Bao, *Adv. Mater.* **2019**, *31*, 1902869.

[74] W. Wang, J. Liu, H. Li, Y. Zhao, R. Wan, Q. Wang, J. Xu, B. Lu, *Adv. Sci.* **2025**, *12*, 2414834.

[75] D. Won, J. Kim, J. Choi, H. Kim, S. Han, I. Ha, J. Bang, K. K. Kim, Y. Lee, T.-S. Kim, J.-H. Park, C.-Y. Kim, S. H. Ko, *Sci. Adv.* **2022**, *8*, abo3209.

[76] X. Xie, Z. Xu, X. Yu, H. Jiang, H. Li, W. Feng, *Nat. Commun.* **2023**, *14*, 4289.

[77] H. Yuk, B. Lu, S. Lin, K. Qu, J. Xu, J. Luo, X. Zhao, *Nat. Commun.* **2020**, *11*, 1604.

[78] C. M. Tran, Z. Yue, C. Qin, K. B. C. Imani, M. Dottori, R. J. Forster, G. G. Wallace, *Adv. Mater.* **2025**, *37*, 2507779.

[79] H. Honaryar, S. Amirfattahi, Z. Niroobakhsh, *Small* **2023**, *19*, 2206524.

[80] G. Chen, X. Liang, P. Zhang, S. Lin, C. Cai, Z. Yu, J. Liu, *Adv. Funct. Mater.* **2022**, *32*, 2113262.

[81] Y. Zheng, Y. Wang, F. Zhang, S. Zhang, K. D. Piatkevich, N. Zhou, J. K. Pokorski, *Adv. Mater. Technol.* **2022**, *7*, 2101514.

[82] K. Unger, F. Greco, A. M. Coclite, *Adv. Mater. Technol.* **2022**, *7*, 2100717.

[83] B. Yan, S. Liu, Y. Yuan, X. Hou, M. Zhou, Y. Yu, Q. Wang, C. He, P. Wang, *Adv. Funct. Mater.* **2024**, *34*, 2401097.

[84] X. Meng, L. Mo, S. Han, J. Zhao, Y. Pan, F. Wang, Y. Fang, L. Li, *Adv. Mater. Interfaces* **2023**, *10*, 2201927.

[85] C. Zhu, A. Chortos, Y. Wang, R. Pfattner, T. Lei, A. C. Hinckley, I. Pochorovski, X. Yan, J. W. F. To, J. Y. Oh, J. B. H. Tok, Z. Bao, B. Murmann, *Nat. Electron.* **2018**, *1*, 183.

[86] Y. Wang, C. Zhu, R. Pfattner, H. Yan, L. Jin, S. Chen, F. Molina-Lopez, F. Lissel, J. Liu, N. I. Rabiah, Z. Chen, J. W. Chung, C. Linder, M. F. Toney, B. Murmann, Z. Bao, *Sci. Adv.* **2017**, *3*, 1602076.

[87] S. Sekine, Y. Ido, T. Miyake, K. Nagamine, M. Nishizawa, *J. Am. Chem. Soc.* **2010**, *132*, 13174.

[88] Y. Ido, D. Takahashi, M. Sasaki, K. Nagamine, T. Miyake, P. Jasinski, M. Nishizawa, *ACS Macro Lett.* **2012**, *1*, 400.

[89] X. Du, H. Wang, Y. Wang, Z. Cao, L. Yang, X. Shi, X. Zhang, C. He, X. Gu, N. Liu, *Adv. Mater.* **2024**, *36*, 2403411.

[90] D. Won, H. Kim, J. Kim, H. Kim, M. W. Kim, J. Ahn, K. Min, Y. Lee, S. Hong, J. Choi, C. Y. Kim, T.-S. Kim, S. H. Ko, *Nat. Electron.* **2024**, *7*, 475.

[91] Y. Li, H. Zhou, H. Yang, K. Xu, *Nano-Micro Lett.* **2024**, *17*, 57.

[92] Y. Xue, J. Zhang, X. Chen, J. Zhang, G. Chen, K. Zhang, J. Lin, C. Guo, J. Liu, *Adv. Funct. Mater.* **2021**, *31*, 2106446.

[93] Y. Liu, J. Li, S. Song, J. Kang, Y. Tsao, S. Chen, V. Mottini, K. McConnell, W. Xu, Y.-Q. Zheng, J. B. H. Tok, P. M. George, Z. Bao, *Nat. Biotechnol.* **2020**, *38*, 1031.

[94] J. Park, H. W. Kim, S. Lim, H. Yi, Z. Wu, I. G. Kwon, W.-H. Yeo, E. Song, K. J. Yu, *Adv. Funct. Mater.* **2024**, *34*, 2313728.

[95] K. Zhang, X. Chen, Y. Xue, J. Lin, X. Liang, J. Zhang, J. Zhang, G. Chen, C. Cai, J. Liu, *Adv. Funct. Mater.* **2022**, *32*, 2111465.

[96] S. J. Wu, X. Zhao, *Chem. Rev.* **2023**, *123*, 14084.

[97] F. Liu, X. Liu, F. Chen, Q. Fu, *Prog. Polym. Sci.* **2021**, *123*, 101472.

[98] X. Wang, X. Sun, D. Gan, M. Soubrier, H.-Y. Chiang, L. Yan, Y. Li, J. Li, S. Yu, Y. Xia, K. Wang, Q. Qin, X. Jiang, L. Han, T. Pan, C. Xie, X. Lu, *Matter* **2022**, *5*, 1204.

[99] H. Yuk, C. E. Varela, C. S. Nabzdyk, X. Mao, R. F. Padera, E. T. Roche, X. Zhao, *Nature* **2019**, *575*, 169.

[100] A. Inoue, H. Yuk, B. Lu, X. Zhao, *Sci. Adv.* **2020**, *6*, aay5394.

[101] H. Tang, Y. Li, S. Liao, H. Liu, Y. Qiao, J. Zhou, *Adv. Healthcare Mater.* **2024**, *13*, 2400562.

[102] J. Zheng, J. Fang, D. Xu, H. Liu, X. Wei, C. Qin, J. Xue, Z. Gao, N. Hu, *ACS Nano* **2024**, *18*, 15332.

[103] X. Yang, W. Chen, Q. Fan, J. Chen, Y. Chen, F. Lai, H. Liu, *Adv. Mater.* **2024**, *36*, 2402542.

[104] N. Li, S. Kang, Z. Liu, S. Wai, Z. Cheng, Y. Dai, A. Solanki, S. Li, Y. Li, J. Strzalka, M. J. V. White, Y.-H. Kim, B. Tian, J. A. Hubbell, S. Wang, *Nat. Mater.* **2025**, *1*.

[105] Y. Jiang, A. A. Trotsuk, S. Niu, D. Henn, K. Chen, C.-C. Shih, M. R. Larson, A. M. Mermin-Bunnell, S. Mittal, J.-C. Lai, A. Saberi, E. Beard, S. Jing, D. Zhong, S. R. Steele, K. Sun, T. Jain, E. Zhao, C. R. Neimeth, W. G. Viana, J. Tang, D. Sivaraj, J. Padmanabhan, M. Rodrigues, D. P. Perrault, A. Chattopadhyay, Z. N. Maan, M. C. Leeolou, C. A. Bonham, S. H. Kwon, et al., *Nat. Biotechnol.* **2023**, *41*, 652.

[106] Y. Lan, K. Yao, P. Shi, Y. Xue, J. Liu, *Small Methods* **2025**, *9*, 01142.

[107] Y. Feng, L. Shan, Y. Wang, X. Chen, C. Wang, J. Liu, *ACS Nano* **2025**, *19*, 16675.

[108] L. Shan, Y. Xue, X. Chen, Y. Wang, Y. Feng, L. Dong, C. Wang, P. Zhang, F. Wang, L. Guo, J. Liu, *Adv. Mater.* **2025**, *11014*.

[109] Z. Shen, Z. Zhang, N. Zhang, J. Li, P. Zhou, F. Hu, Y. Rong, B. Lu, G. Gu, *Adv. Mater.* **2022**, *34*, 2203650.

[110] F. Mo, P. Zhou, S. Lin, J. Zhong, Y. Wang, *Adv. Healthcare Mater.* **2024**, *13*, 2401503.

[111] J. Wu, H. Liu, W. Chen, B. Ma, H. Ju, *Nat. Rev. Bioeng.* **2023**, *1*, 346.



Yu Xue received his Ph.D. degree at Southern University of Science and Technology and currently works in Jiangxi Science and Technology Normal University. His research interests focus on the design and fabrication of functional hydrogels toward bioelectronic interface.



Zhipeng Ni received his Ph.D. degree at Zhejiang University and currently work as a postdoc at Southern University of Science and Technology. His research interests focus on the hydrogels and interface engineering for tissue repair.



Yafei Wang received his Ph.D. from Harbin Institute of Technology and is currently an Associate Research Fellow at Southern University of Science and Technology. His research focuses on the mechanics of flexible and active materials, with particular interest in buckling instability and morphoelasticity, applied to functional metamaterials and adhesive interfaces.



Liangjie Shan is a Ph.D. candidate at the Department of Mechanical and Energy Engineering, Southern University of Science and Technology. His research interests center on the design and synthesis of functional hydrogels toward bioelectronic interface.



Ji Liu is currently an Associate Professor in the Department of Mechanical and Energy Engineering, Southern University of Science and Technology. He obtained his Ph.D. from the University of Liege (Belgium) and University of Bordeaux (France). Prior to joining SUStech, he conducted post-doc research in the University of Cambridge, Massachusetts Institute of Technology and Harvard Medical School. His research interest is to design and fabricate functional hydrogels and hydrogels-based electronics for biointerfacing.